International Journal of Earth Sciences (2023) 112:459–488
https://doi.org/10.1007/s00531-022-02263-5

ORIGINAL PAPER

Architecture of Eastern Mediterranean sea rifted margins: observations and uncertainties on their Mesozoic evolution

M. Nirrengarten[1] · G. Mohn[1] · F. Sapin[2] · C. Nielsen[2] · A. McCarthy[1,3] · J. Tugend[1]

Received: 9 July 2021 / Accepted: 25 October 2022 / Published online: 22 November 2022

Abstract
The geodynamic evolution of the East Mediterranean Sea (EMS) in the Mesozoic remains a "Gordian knot" tying together the Atlantic and Tethys oceanic systems. A key to unravel its complex evolution resides in determining the structure and formation age of its passive margins. Here, we investigate the Mesozoic architecture of different segments of the southern passive margin of the EMS using 2D and 3D seismic data combined with stratigraphic observations and gravity anomaly maps. Based on these offshore datasets, a new structural rift domain map of the eastern EMS is proposed showing the distribution of different crustal domains. Regional cross sections from the Western Desert to the northern Levant passive margins systematically show a sharp crustal neck of the EMS passive margins passing laterally in less than 30 km from moderately thinned continental crust (20–25 km thick) overlain by post-rift carbonate platform to distal deep basin (top basement > 8 s TWT). This sharp crustal thinning observed on both the southern and eastern margins of the EMS hampers the unambiguous identification of transform passive margin segments from orthogonal ones. The age of rifting and spreading of the different EMS basins are only partially constrained by boreholes and seismic correlation. To reduce uncertainties, we analyze and integrate the stratigraphic rift record from onshore former conjugate margins, which are now integrated in the Alps, Balkanides, Hellenides and Taurides belts on the northern side of the EMS. With this offshore/onshore approach, we identified the spatial and temporal evolution of rifting and spreading activity around EMS, highlighting poly-phased and poly-directional events from the Permian to the Cretaceous. We show that two competing geodynamic engines controlled extensional processes in the EMS: the opening of the Central Atlantic since the Late Triassic to the southwest and the evolution of multiple subduction zones in the Tethys domain to the northeast.

Keywords Eastern Mediterranean sea · Rifted margins · Seismic interpretation · Rift domain mapping

Introduction

From the Late Paleozoic to the Cenozoic, the Tethys domain represented an assemblage of multiple oceanic branches, rifted basins, micro-continents and convergent plate boundaries, forming a V-shape realm between Gondwana and Eurasia continents (Şengör and Yilmaz 1981; Robertson et al. 2007). Almost all of the distinct segments of the Tethys domain were subsequently subducted or integrated in the wide Tethyside orogenic complex that runs from Western Europe to SE Asia (Sengor 1990; van Hinsbergen et al. 2020). The geodynamic evolution of the Tethys domain is therefore mostly based on the analysis of different orogenic belts (e.g., Alps, Hellenides, Dinarides, Pontides, Taurides. Figure 1). However, the southern and eastern rifted margins of the Eastern Mediterranean Sea (EMS) (Fig. 1) remain relatively intact and provide the most relevant clues on the mechanisms of Tethyan rifting and breakup (Robertson 2007; Gardosh et al. 2010; Frizon de Lamotte et al. 2011). There is a general consensus that EMS developed along the northern margin of Gondwana and led to the separation of the Greater Adria continent (formed by Apulia/Adria, Pelagonia and Taurus continental blocks; Van Hinsbergen et al. 2020). However, the geodynamic processes related to the opening of the EMS are still strongly debated (e.g. Dercourt

✉ M. Nirrengarten
michael.nirrengarten@cyu.fr

[1] Département Géosciences et Environnement, CY Cergy Paris Université, MIR Neuville Sur Oise, Cergy, France

[2] Totalenergies, Centre Scientifique et Technique Jean Féger (CSTJF), Avenue Larribau, 64000 Pau, France

[3] Institute of Geochemistry and Petrology, ETH Zürich, 8092 Zurich, Switzerland

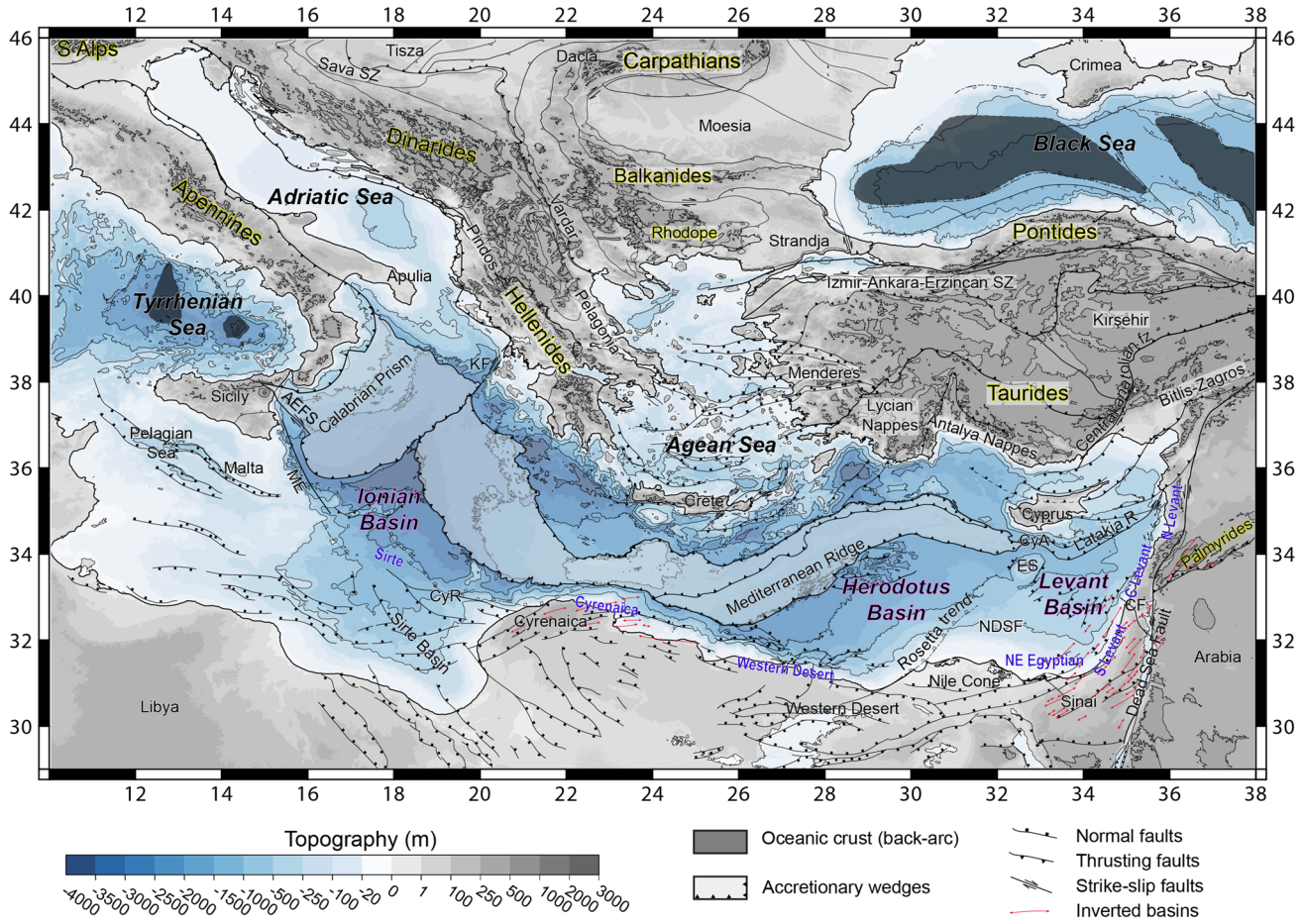

Fig. 1 Simplified structural map of the EMS and surrounding regions (compiled after Chamot-Rooke et al. 2005; Faccenna et al. 2014; Frizon de Lamotte et al. 2011; Ghalayini et al. 2018; Tassy et al. 2015). The topographic base map originated from Etopo1 (Amante and Eakins 2009). Yellow surroundings indicate orogenic belts, pink surroundings correspond to the Mesozoic basins, blue color font indicates the different margin segments. AEFS: Alfeo-Etna Fault system; CF: Carmel Fault; CyA: Cypruc Arc; CyR: Cyrenaica Ridge ES: Eratosthenes Seamount; KF: Kefalonia Fault; ME: Malta Escarpment, NDSF: Nile Deep Sea Fan

et al. 1993; Stampfli and Borel 2002; Le Pichon et al. 2019; van Hinsbergen et al. 2020). The use of distinct geological and geophysical datasets has led to markedly contrasting interpretations on the timing of opening of the different basins of EMS (ranging from Carboniferous to Cretaceous), its structural evolution (divergent to transform segments) and kinematics (NNE-SSW to WNW-ESE extension) (Ben-Avraham et al. 2006; Granot 2016; Segev et al. 2018; van Hinsbergen et al. 2020).

In contrast to the former Greater Adria rifted margins, which are currently dismembered and located in different orogenic belts North of the EMS (Fig. 1), the southern and eastern EMS rifted margins, from the Malta Escarpment to the West to Syria to the East, are relatively well preserved from significant extensional and compressional reactivations in the Cretaceous and Cenozoic (Ben-Avraham and Grasso 1991; Bosworth et al. 1999, 2008; Sagy et al. 2018). However, the EMS is affected by several post-breakup events, such as, Mesozoic carbonate platforms built-up, gentle folds (Allen et al. 2016), deposition of thick Cenozoic deltaic sequences (particularly offshore the Nile Cone Figs. 1, 2), thick evaporite and salt sequences related to the Messinian crisis, gravity-driven tectonic structures, as well as vertical motion in relation to mantle dynamics (Faccenna et al. 2014) that hamper unequivocal interpretation of basement structures of the EMS rifted margins. Our innovative strategy to unravel the eastern EMS opening (East of the Mediterranean Ridge Fig. 2) is to optimize seismic interpretation by the identification and mapping of key structural elements on multiple dense 2D and 3D seismic surveys imaging subsurface down to 14 s TWT (Fig. 3). Seismic observations are interpreted together with gravity anomaly maps to present a structural rift domain map of the easternmost part of the EMS (Figs. 2, 3, 4). Rift domain maps show the distribution of different crustal domains of passive margins (Tugend et al. 2014, 2015a) and can be used to constrain palinspastic

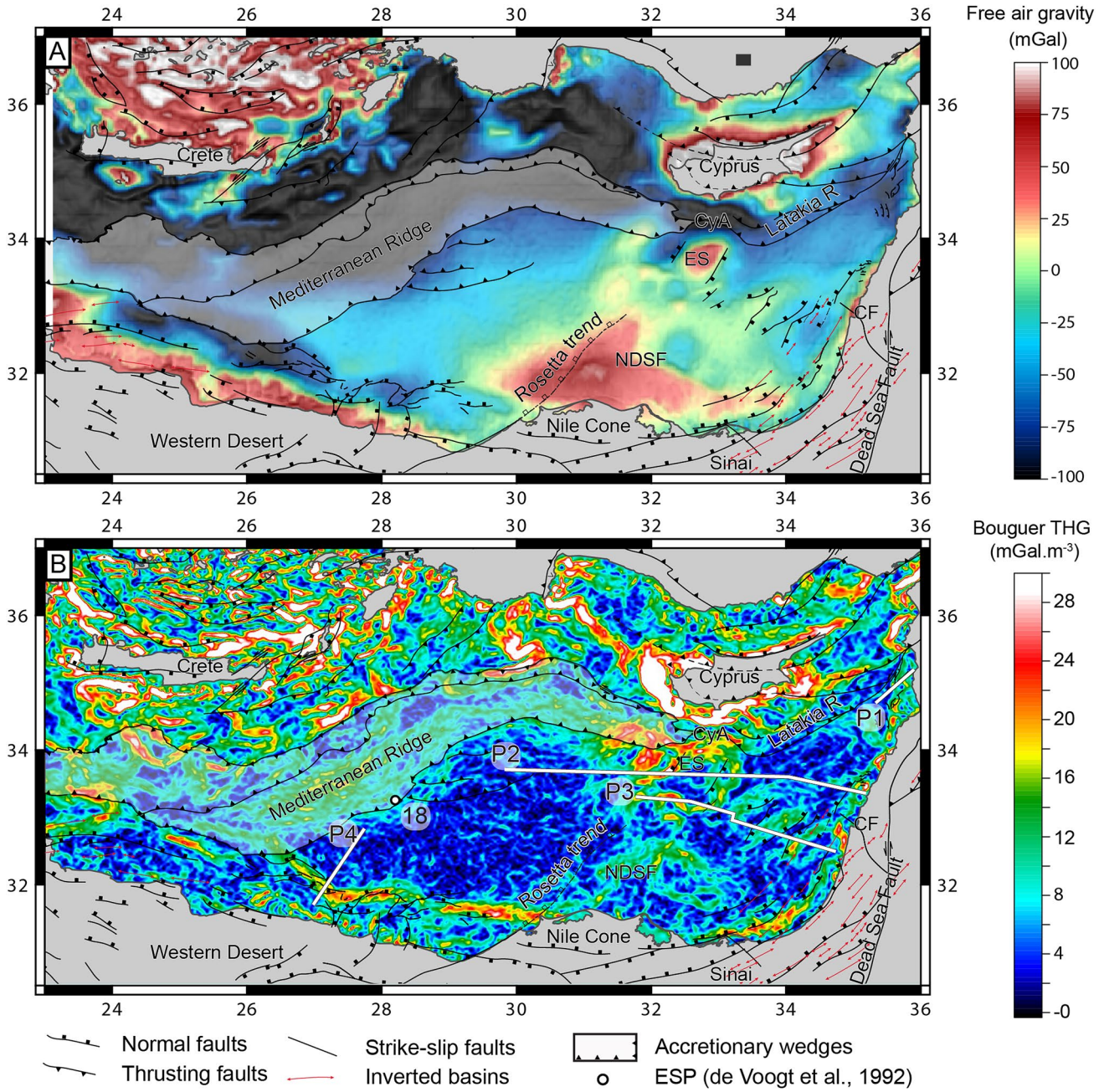

Fig. 2 **A** Free air gravity map (Sandwell et al. 2014) and **B** Total Horizontal Gradient (THG) of the Bouguer gravity anomaly from the Eastern Mediterranean Sea. The location of the seismic profile is indicated. P1 to P4 are respectively shown on Figs. 6, 7, 8, 9. CF: Carmel Fault; CyA: Cyprus Arc; ES: Eratosthenes Seamount; ESP: expanding spread profiles; NDSF: Nile Deep Sea Fan

plate models of rift systems (Tugend et al. 2015b; Nirrengarten et al. 2018; Peace et al. 2019). We selected and interpreted four composite seismic sections from various locations and orientations that show the abrupt structure of the preserved EMS passive margins. Offshore, borehole calibrations constrained the post-rift series but were frequently unable to constrain the base of these series (Beydoun 1977; Gardosh and Tannebaum 2014; Tassy et al. 2015), leading to insufficient constraints on the spatial and temporal evolution of rifting and spreading. We therefore integrate a focused review on the rift events recorded in the tectonics unit integrated in the Eurasian fold and thrust belts (Schmid et al. 2020) to better constrain the timing of extensional deformation that shaped the EMS passive margins and different sub-basins. The results of this original offshore/onshore approach are analyzed in light of global plate motion to

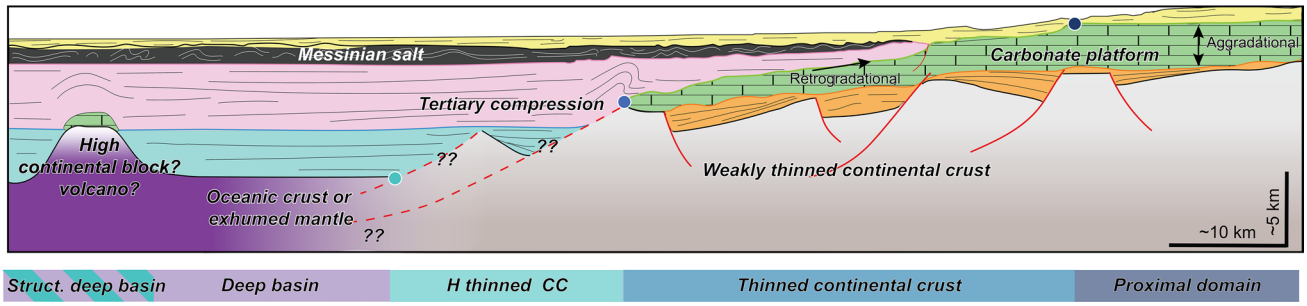

Fig. 3 Schematic cross section showing the main structural elements observed across the EMS of rifted margins. Rift domains are defined based on the seismic determination of key elements represented by the different shades of blue dots. Each domain boundary (shaded blue dot) is discussed in Sect. 3. H Thinned CC: Highly thinned continental crust

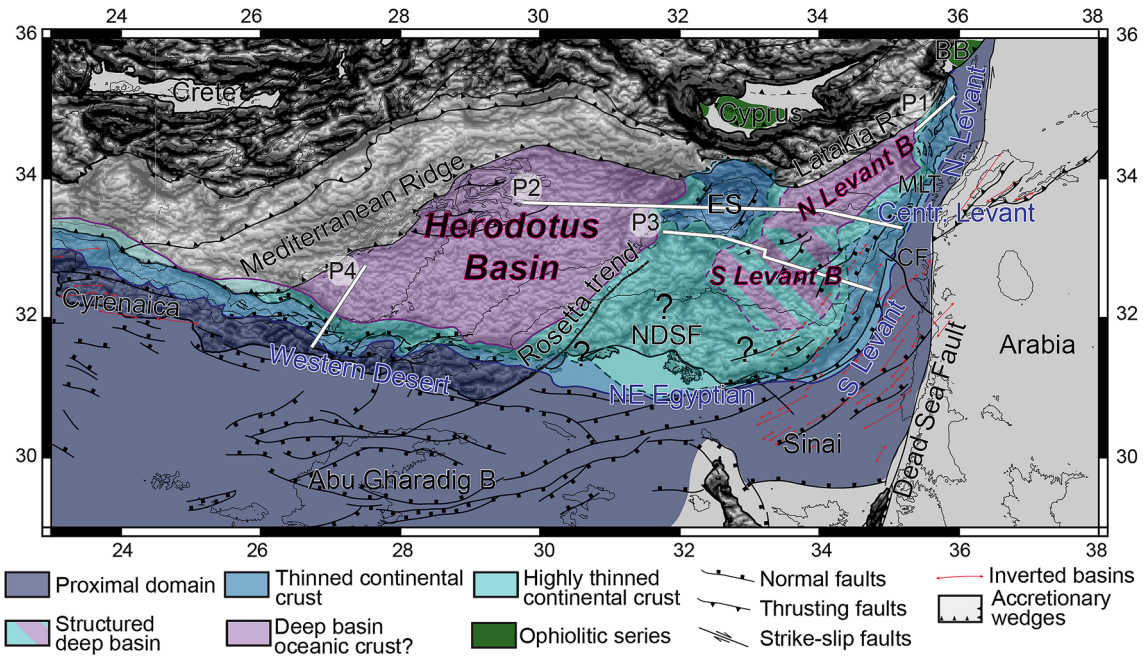

Fig. 4 Rift domain map of the Easternmost Mediterranean Sea overlaying the THG shaded relief grid. The location of the seismic profile is indicated. P1 to P4 are respectively shown on Figs. 6, 7, 8, 9. Pink surroundings correspond to the Mesozoic deep basins, Blue color font indicate the investigated margins. CF: Carmel Fault; ES: Eratosthenes Seamount; MLT: Mount Lebanon Thrust; NDSF: Nile Deep Sea Fan

determine the geodynamic engines responsible for the EMS extensional evolution.

Geological setting

In between Africa and Eurasia, the Mediterranean Sea domain presents heterogeneous topography and bathymetry reflecting the complex spatial and temporal interaction of a variety of tectonic processes (Fig. 1). At present, the EMS domain is a seismogenic zone comprising active strike slip (e.g. Dead Sea Fault Fig. 1) and convergent plate boundaries (e.g. Mediterranean Ridge, Calabrian Prism Fig. 1) (McKenzie 1972). GPS data highlight the northward motion of Arabia, the westward motion of Anatolia and the slab subduction below the Mediterranean Ridge and Calabrian Prism (Reilinger et al. 2006; Palano et al. 2012). The EMS can be subdivided from north to south into three distinct structural domains: 1) accretionary prisms (Calabrian Prism, the Mediterranean Ridge and the Cyprus arc), 2) deep basins (Ionian, Herodotus and Levant basins), 3) rifted continental passive margins (Fig. 1). From the northwest to the southeast of the EMS, the Calabrian Prism, the Mediterranean Ridge and the Cyprus arc form a convergent plate boundary where northern Africa subducts below Eurasia (Dewey and Bird 1970; Jolivet et al. 2003) (Fig. 1). The EMS is formed of

three main deep basins highlighted by bathymetric and free air gravity maps (Figs. 1, 2A). To the west, the Ionian Basin is subducting below the Calabrian Prism and the Mediterranean Ridge (Fig. 1). The Herodotus Basin, located east of the Mediterranean Ridge and offshore Western Desert, is separated from the Levant Basin by the Nile Deep Sea Fan (north of the Nile Cone, Fig. 1) and the Eratosthenes Seamount (south of Cyprus and Latakia Ridge, Fig. 1). Preserved EMS rifted margins (divergent, transform or oblique) are found along northeastern Africa and northwestern Arabia plates, spanning over 2400 km and are separated in different segments (Fig. 1). From West to East, rifted margins are found along the Malta Escarpment, the Sirte Basin and margin, the Cyrenaica margin, the Western Desert margin, the northeast Egyptian margin and the entire Levant margin (Fig. 1) (note that these rifted margins are detailed in Sect. 4).

The oldest known building block of the EMS includes continental lithosphere derived from the collision of the Saharan metacraton with the Arabia Nubian Shield during the Neoproterozoic East African Orogeny (Fritz et al. 2013) (**SM1**). Subsequently, the northern domain of this continental block was affected by the Late Neoproterozoic Cadomian orogeny and back-arc magmatism (Avigad et al. 2016) (SM1). The Paleozoic evolution of the Northern African-Arabian domain is characterized by the deposition of siliciclastic sequences at the northern margin of Gondwana (Avigad et al. 2003). An "arch and basin" geometry formed at that time in response to different thermal and extensional events which caused polygenic unconformities often wrongly unified as the "Hercynian Unconformity" (Frizon De Lamotte et al. 2015). Indeed, most of the domain is outside of the Carboniferous Variscan orogen which can be found further West in Morocco and on the Eurasia continent (Matte 2001). The Herodotus Basin has been suggested to be of oceanic nature and as old as Carboniferous based on loosely defined geomagnetic timescale (Granot 2016) and related to the Variscan orogeny dynamic (Stephan et al. 2019). However, no evidence for this early opening has been described from the sedimentary record neither offshore nor onshore. In contrast, Permian basins are widespread and can be found in the Palmyrides (Syria), Sicily and Crete (Fig. 1) (Brew et al. 2001; Robertson 2006). The tectonic context of these basins is still poorly understood but pelagic carbonates are observed in central Sicily and interpreted as deposited during a widespread episode of continental rifting (Basilone et al. 2016).

The evolution of the EMS in Neoproterozoic and Paleozoic implies that multiple tectonic events are superimposed on each other. Hence, assessing different generations of inheritance in the geological record is crucial to constrain the evolution and inferred age of formation of these rifted margins (Buiter and Torsvik 2014; Petersen and Schiffer 2016). During the Mesozoic, poly-phased rifting, breakup and seafloor spreading characterize the evolution of the Western Tethys. In particular, four key periods have been identified: 1) Middle Triassic (Meliata, Maliac, Balkan Neo-Tethys oceans) (Kozur 1991; Ferrière et al. 2012), 2) Late Triassic (Pindos, Southern Neo-Tethys branch, EMS) (Şengör et al. 1984; Robertson et al. 1996), 3) Early/Mid Jurassic (EMS, Alpine Tethys) (Gardosh et al. 2010; Frizon de Lamotte et al. 2011), 4) Cretaceous (EMS, Levant Basin) (Dercourt et al. 1993; Segev et al. 2018). Specifically, the timing of opening of the EMS, its structural evolution (divergent to transform segments) and kinematics (NNE-SSW to WNW-ESE extension) remain largely debated. For instance, based on crustal thickness maps determined by gravity inversion, Cowie and Kusznir (2012a) suggested that the whole Levant margin is an orthogonal margin while the Western Desert margin represents a transform margin (Fig. 1). In contrast, Schattner and Ben Avraham (2007), based on morphological criteria, interpreted the northern and central Levant margin as a transform margins (North of the Carmel Fault CF Figs. 1, 2). Along the western rim of the EMS, the NW–SE oriented Malta Escarpment (ME, Fig. 1) has recently been interpreted as a paleo transform margin by wide-angle and reflection seismic imaging (Fig. 1) (Dellong et al. 2018; Tugend et al. 2019) suggesting a perpendicular (NE-SW) oriented spreading system. Geodynamic models also differ in terms of directions and age of EMS opening: Stampfli and Borel (2004) proposed a Permian opening in a direction parallel to the Levant margin. Van Hinsbergen et al. (2020) and Dercourt et al. (1986) supported an opening in such a direction, but at markedly distinct time intervals, namely Late Triassic-Early Jurassic and Early–middle Cretaceous respectively. Although the global plate model of Müller et al. (2019) does not integrate the complexity of the EMS opening, a trans-tensional opening is assumed, based on the motion of NE Africa relative to Eurasia. This trans-tensional motion is in accordance with Frizon de Lamotte et al. (2011) and Le Pichon et al. (2019), who proposed that the northern African margin is a transform or highly oblique margin active in the Jurassic and even Cretaceous and related to the opening of the Central Atlantic. Recently, Jagger et al. (2020) proposed a poly-phased and poly-directional rifting and breakup leading to a Middle Triassic to Middle Jurassic (240–170 Ma) breakup/opening of the easternmost domain of the EMS (Levant-Herodotus basins Fig. 1) and a Late Jurassic to mid Cretaceous (145–93 Ma) opening of the western part of the EMS (Ionian Basin) (Fig. 1).

Compressional tectonic started during the Cretaceous Magnetic Quiet Period (~ 120–84 Ma) in EMS as a consequence of the opening of the Equatorial Atlantic and the northeastward motion of Africa (Dewey et al. 1989; Rosenbaum et al. 2002) leading to the subduction of the northern EMS oceanic crust below the different accretionary systems (Menant et al. 2016). In addition, fold structures are

observed on the southern Levant and Cyrenaica margins and are related to far field deformation named Syrian Arc phase, which initiated at ca. 80 Ma. (Fig. 1) (Arsenikos et al. 2013; Sagy et al. 2018). Contrary to the southern margin of the EMS which was little affected by compression, the northern margin collided with the southern Eurasia margin, leading to the incorporation of dismembered rift structures in folds and thrusts belts (Schmid et al. 2020) (Fig. 1, SM2). In certain instances, these rifted margins were partly subducted, as highlighted by the Plattenkalk unit (Crete) which contains Mesozoic passive margin sequences metamorphosed to high pressure in the Miocene (8–10 kbar, 300–400 °C, Ring et al. 2001). However, despite complex and variably intense Cretaceous and Cenozoic orogenic overprints, Mesozoic stratigraphic records and ophiolitic belts can still be recognized on the Balkan and Anatolian Peninsulas, providing key information to constrain rifting, spreading and subduction dynamic of the EMS (see review of Schmid et al. 2020).

In the Tertiary, thick (> 4 km) siliciclastic sedimentary packages accumulated in the Levant and Herodotus Basins (Hawie et al. 2013). This sedimentary flux originated mostly from the onset of the Nile river system (Macgregor 2012) which was driven by the uplift and denudation of the Afro-Arabian plate induced by the Afar mantle plume in the Late Eocene (Bosworth et al. 2005). More recently, the African-Eurasian convergence reduced the seawater circulation between the Atlantic Ocean and the Mediterranean Sea at the Gibraltar Strait leading to the deposition of evaporitic sequences during the Messinian Salinity Crisis (6–5.3 Ma) (Roveri et al. 2016).

Data and methodology

In this contribution, we adopt an offshore and onshore approach to best constrain the spatial and temporal evolution of the rift and spreading events that shaped the EMS passive margins (Levant, Western Desert) and deep basins (Herodotus, Levant). Offshore, regional composite seismic profiles (Sect. 4) show the Mesozoic stratigraphic architecture and crustal structure of the southern and eastern EMS passive margins. These new interpretations integrate results from existing extensive geophysical surveys in the region as well as available borehole calibrations and stratigraphic correlations. To reduce uncertainties in the interpretation of the deepest parts of the basins, offshore interpretations are completed by the integration of observations from the northern conjugate rifted margins now sampled as remnants in onshore orogenic belts (Sect. 5).

Passive margin crustal architecture alone is insufficient to discriminate between orthogonal and transform segments of the EMS, and hence deduce the kinematics of rifting and spreading events. Offshore and onshore observations are subsequently confronted with existing plate kinematic reconstructions to determine the driving forces responsible for the Mesozoic opening of the EMS and deduce the most probable directions of extension in a global kinematic frame (Sect. 6).

Dataset compilation

The main dataset used in this study consists of industrial 2D and 3D seismic reflection lines extending offshore from the Mediterranean Ridge to the Levant margin (Fig. 1). TotalEnergies provided access to seismic data that were interpreted on a workstation using Sismage software allowing the correlation of the different horizons and structural elements. Although the quality and penetration depth of the seismic profiles is variable, coherent reflection pattern up to 8 s TWT are typically observed. To highlight the main structural elements of EMS rifted margins and capture their lateral variability, we generated and interpreted four composite sections using available stratigraphic correlations (Gardosh et al. 2010; Tassy et al. 2015; Ghalayini et al. 2018). Seismic acquisition parameters are variable for the different selected profiles depending on the company that acquired and processed the data. Data origin is acknowledged in the figure captions.

We also include in our integrated analyses: (1) Published seismic refraction data (Makris et al. 1983; Ben-Avraham et al. 2002; Welford et al. 2015; Feld et al. 2017) to characterize the crustal velocities along different profiles and interpret them as lithologies; (2) Onshore and offshore borehole data (Garfunkel and Derin 1984; Robertson 1998) and (3) Maps of free air gravity (Fig. 2A) and magnetic anomalies (Sandwell et al. 2014; Meyer et al. 2017). Transform gravity grids such as the total horizontal gradient of the Bouguer gravity anomaly (Fig. 2B, THG) that locates the extrema value over the edge of the body (Blakely 1995) are used to extend the mapping of structures when these could not be imaged by seismic reflection and refraction profiles. We also integrate regional structural maps (Chamot-Rooke et al. 2005; Jagger et al. 2020) as well as stratigraphic, metamorphic, petrologic, geochronological and structural data from the EMS western and northern margins which have already been interpreted into tectonic maps (Schmid et al. 2020; van Hinsbergen et al. 2020).

Approach to map structural rift domains in the EMS

The rift mapping methodology is based on the identification of structural elements that characterize different crustal domains of a given passive margin (e.g., main escarpments, carbonate platform edges, structural style, top basement depth and morphology). Here we adapt the mapping methodology developed for hyper-extended magma-poor rifted margin (Peron-Pinvidic et al. 2013; Tugend et al. 2015a)

to the EMS rifted margins. The EMS rifted margins show distinct structural characteristics that can be identified across the different segments as summarized in an idealized section in Fig. 3. The characteristics of the different rift domains are outlined below:

- The *proximal rift domain* is generally characterized by very little to no crustal thinning. The proximal domain can be characterized by its post-rift sedimentary architecture, as carbonate platforms are only aggradational whereas retrogrationnal rimmed platform margins develop on thinner crust (Fig. 3). We therefore map this limit in the style of carbonate platform building as the proximal/ thinned continental crust domain boundary (dark blue dot Fig. 3). Onset of thinning can also be roughly located using a thinning factor map based on gravity inversion based on public domain data (Cowie and Kusznir 2012a) (SM 2). Seismological and gravity modeling show a ~ 30 km thick (continental) crust along Western Desert margin and west of the Dead Sea Fault on the Levant margin (Fig. 1), whereas thicker crust (~ 35 to 40 km) is observed along the Saharan Metacraton and Arabo-Nubian Shield to the south and southeast respectively (Cowie and Kusznir 2012a, b; Sobh et al. 2019) (SM1). This variation in crustal thickness is used to identify the boundary between the proximal domain and undeformed continent.

- The *thinned continental crust domain* is also covered by post-rift Mesozoic carbonate platforms (Tassy et al. 2015). However, the platform is retrogradational through the domain (regression of rimed platform margins) (Fig. 3). With good quality seismic data, multiple normal faults bounding sedimentary wedges can be identified below the post-rift carbonate platform (Fig. 3). The presence of a wide carbonate platform over tens of millions of years suggests a relatively low rate of subsidence and, by implication, relatively low crustal thinning. This is in consistent with a crustal thickness of 20–25 km determined on the few wide-angle seismic profiles available along the Levant margin (Ben-Avraham et al. 2002). The distal edge of the carbonate platform marks the distal boundary of the thinned continental crust (medium blue dot Fig. 3).

- The *highly thinned continental crust domain* corresponds in most cases to a sharp escarpment where the top basement deepens from ~ 4–5 s to > 7 s TWT over a distance of 10 to 30 km. This sharp transition marked by one or two extensional faults likely reflects strong crustal thinning from ~ 20 to 10 km thick or even less (Fig. 3). Post-rift sediments passively onlap the highly thinned crust (in blue, Fig. 3). A calci-detritic slope facies illustrating the destabilization of the platform edge can be identified (e.g. Western Desert margin: Tassy et al. 2015). Tertiary folded structures are preferentially located in this highly thinned continental crust domain (Fig. 3). Such localization of folds is likely a consequence of the sediment package overlying a sharp basement topography (e.g. central Levant margin (Ghalayini et al. 2018)). The transition to the deep basin domain corresponds to a sharp top basement slope break mapped throughout the EMS margins (light blue dot Fig. 3).

- The *deep basin domain* is characterized by a deep top basement (> 7 s TWT). The identification of the top basement is often problematic. For instance, in the Herodotus Basin, well layered sedimentary packages can locally be observed down to 11 s TWT (> 10 km) (Jagger et al. 2020) (Fig. 3). Where inferred, the top basement shows a sub-horizontal morphology (Fig. 3). Sporadic basement highs (~ 10 km in width) are occasionally found within these basins (i.e., structured deep basin) and distinguished on the rift domain map (hatching in Figs. 4 and 5). These distal structures often present gentle folding of the post-rift sequences, whereas pre-existing basements structures such as fault bounded rotated blocks, volcanic seamounts or mud diapirs accompanied (or not) by carbonate build up have been suggested/interpreted (Gardosh et al. 2008; Ben-Gai 2019; Tari et al. 2020) (Fig. 3). The basement nature of the deep basin domain is unclear and could correspond to oceanic crust, exhumed mantle or highly thinned continental crust with possible magmatic additions (de Voogd et al. 1992; Steinberg et al. 2018). Although the nature of the basement is partly unconstrained, this domain accommodated most of the tectonic extension in the EMS.

Rifted margin architecture of the easternmost Mediterranean Sea

This result section presents observations and interpretations along composite seismic sections selected to illustrate the general structure of different segments the EMS passive margins. The identification of rift domains is presented on maps (Figs. 4, 5) and illustrated by four regional seismic cross sections across different margin segments (Figs. 6, 7, 8, 9) that provide key structural elements to unravel the tectonic evolution of the EMS. Significant uncertainties remain for the stratigraphic interpretation of the deep basins due to the lack of deep wells. For each segment, first order observations are summarized and followed by their interpretation.

Levant margin and basin

The Levant margin forms the easternmost rim of the EMS (Figs. 1, 4). This NNE-SSW oriented rifted margin runs from the Latakia ridge to the northern Sinai where the coast changes its orientation to E-W (Figs. 1, 4). We divide the Levant margin into three segments, namely southern, central and northern segments while in the deepest part, the northern and southern deep Levant basins are distinguished (Fig. 4).

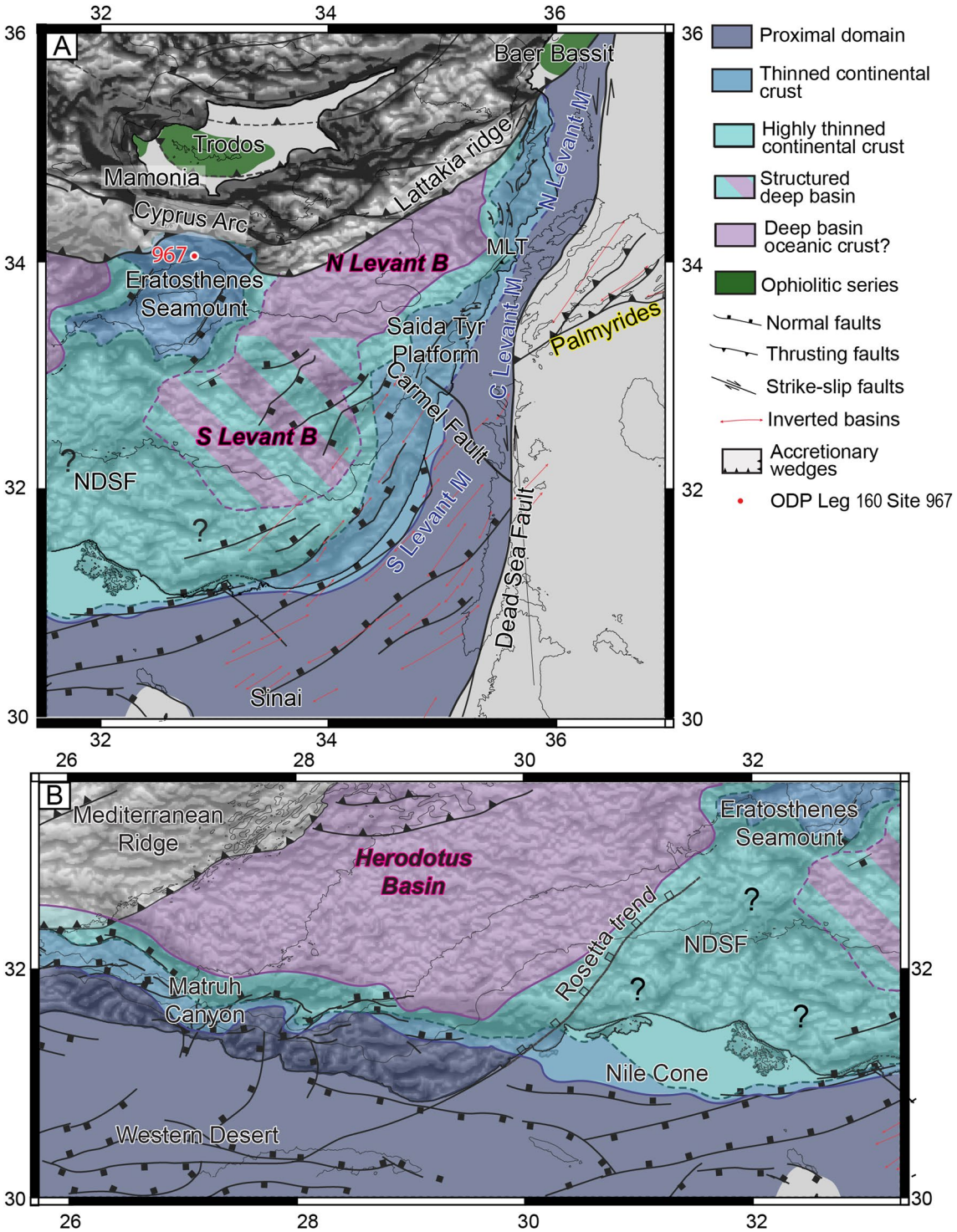

Fig. 5 **A** Rift domain map of Levant margins system **B** Rift domain map of the Western Desert and NE Egyptian margins. Yellow surroundings indicate orogenic belts, Pink surroundings correspond to the Mesozoic deep basins, Blue color font indicates the investigated margins. B: Basin MLT: Mount Lebanon Thrust; NDSF: Nile Deep Sea Fan

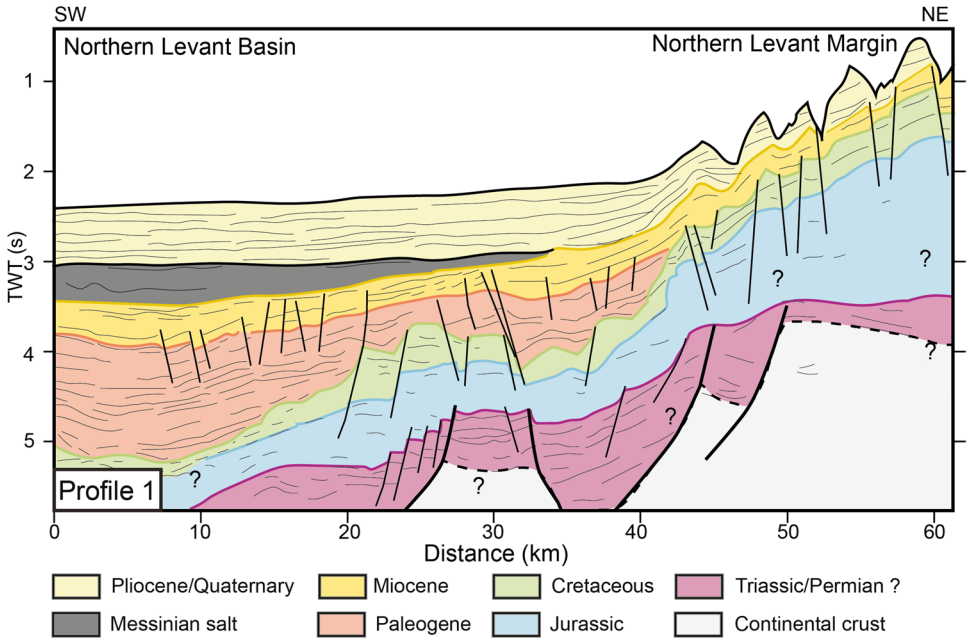

Fig. 6 Interpreted seismic section line A crossing the northern Levant margin (adapted from Bowmann 2011). Black dashed line corresponds to the interpreted top basement

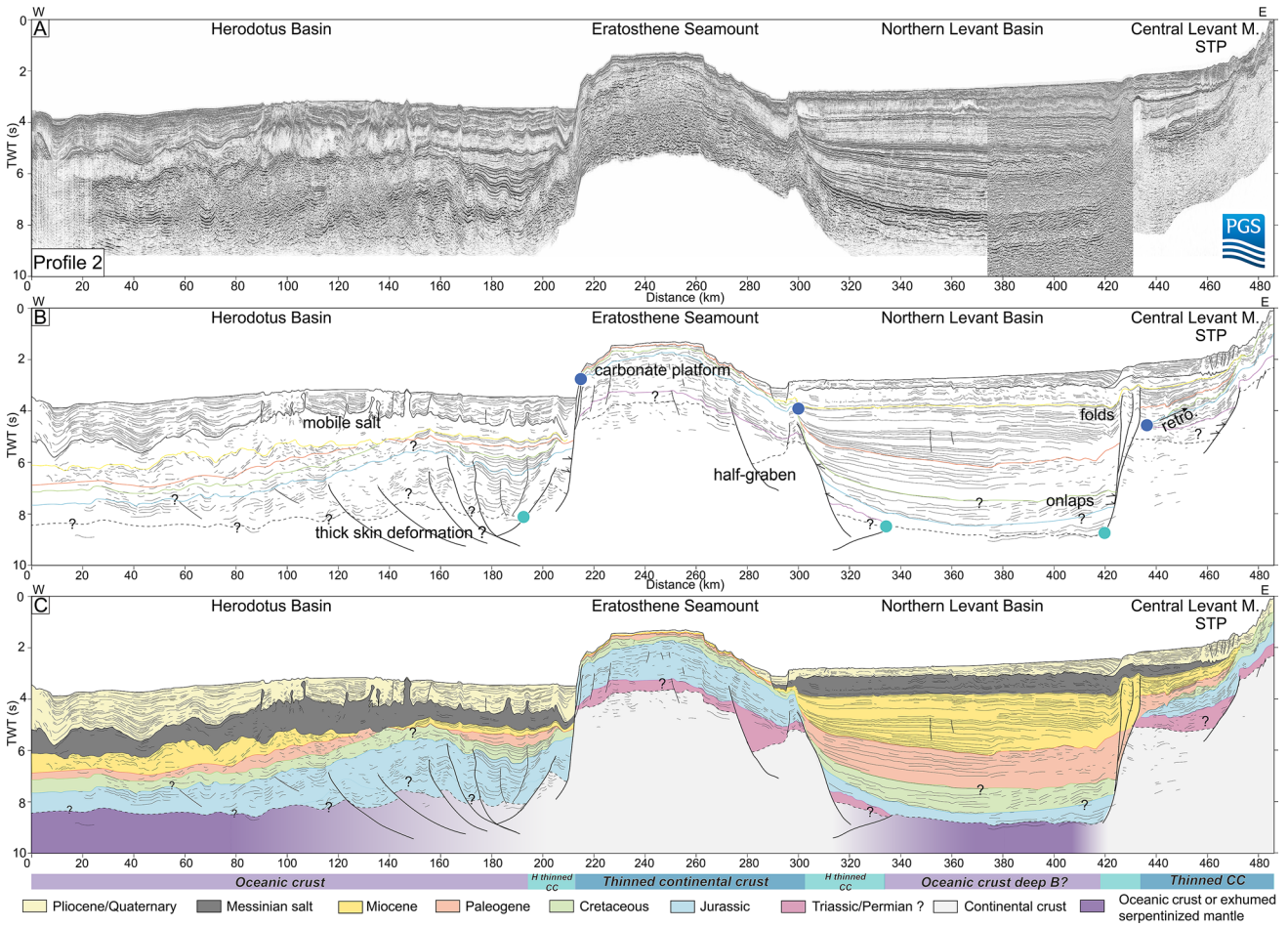

Fig. 7 **A** Un-interpreted composite seismic line B running from the Central Levant Margin to the Herodotus Basin. **B** Line drawing of line B highlighting the main horizons **C** Structural interpretation of line B with the associated rift domains. Black dashed line corresponds to the interpreted top basement. STP: Saïda-Tyr Platform. (Data courtesy of PGS)

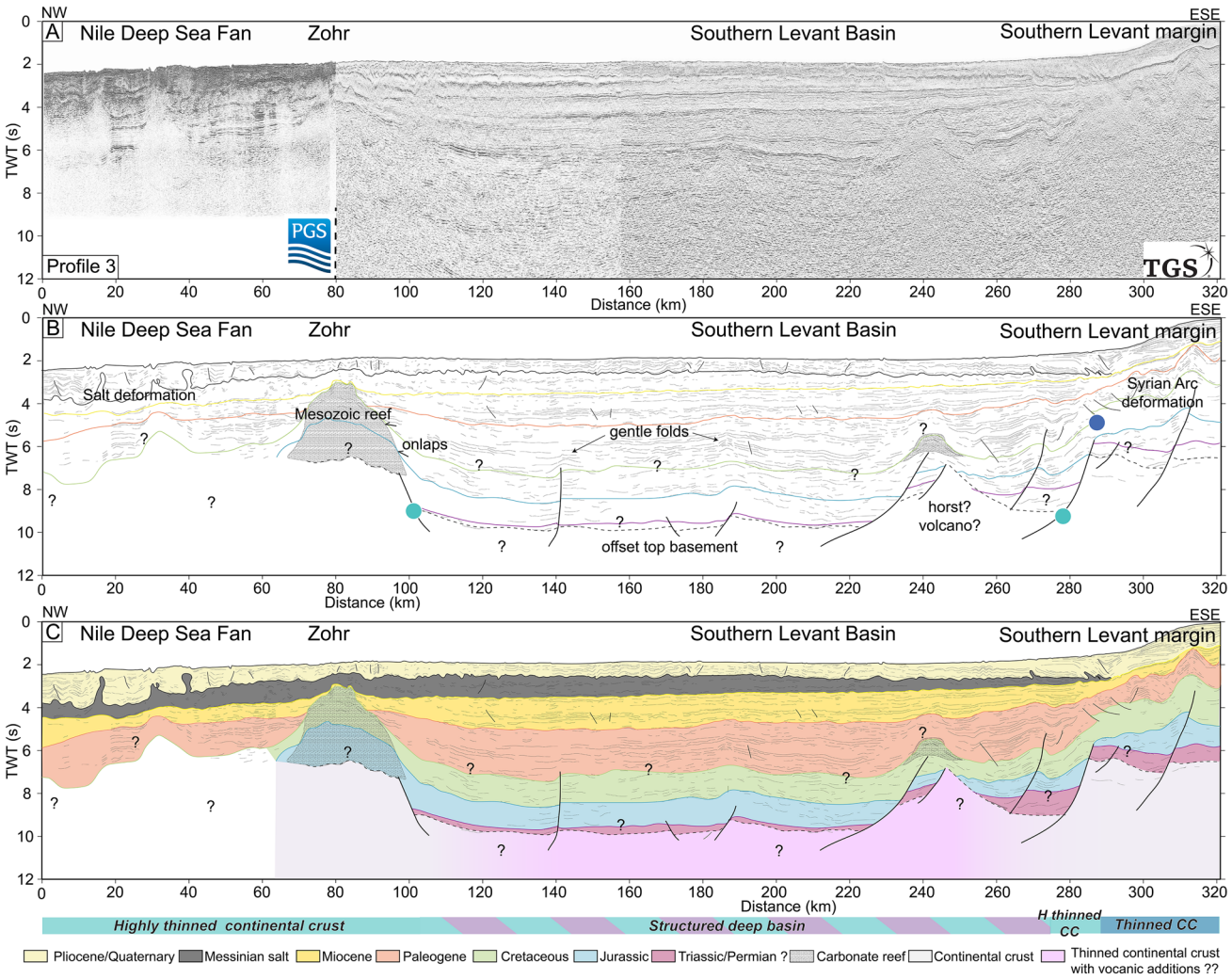

Fig. 8 **A** Un-interpreted composite seismic line C running from the southern Levant Margin to the Herodotus Basin. **B** Line drawing of line C highlighting the main horizons **C** Structural interpretation of line C with the associated rift domains (Data courtesy of TGS and PGS)

Northern Levant margin

The northern segment of the Levant margin is bounded to the north by the NE-SW striking Latakia ridge, a branch of the Cyprus arc subduction system which has been active, albeit not continuously, from the Late Cretaceous to the present-day (Symeou et al. 2018). The Baër-Bassit ophiolite (BB, Fig. 4), which is located to the west of Syria, is the onshore continuation of this convergent system (Fig. 5). It is formed of dismembered Late Triassic to Cretaceous deep-water facies sediments of the Baër-Bassit mélange (base slope facies) and is located structurally below the Late Cretaceous supra-subduction Baër-Bassit ophiolites (Al-Riyami and Robertson 2002) indicating at least two extensional phases. The architecture of the northern Levant margin is strongly affected by Late Cretaceous Cyprus arc convergent system (Symeou et al. 2018) which places the margin in a foreland context (Bowman 2011). Although affected by compression, tilted rift structures can still be identified (Bowman 2011). In the northern Levant margin segment, the edge of the Mesozoic carbonate platform (interpreted boundary between the thinned and highly thinned continental crust domains, Fig. 3) evolves from being NNE-SWW oriented to the north (between latitude 35.7° and 34.6°) to being NNW-SSE oriented further south (between latitude 34.6° and 34°) (Fig. 4, 5). Our description of the northern Levant margin structure focuses along a NE-SW oriented section (Fig. 6) located in the NNE-SSW oriented segment (Fig. 4).

Delimitation and description of structural rift domains The *proximal* and *thinned continental domains* are characterized by the presence of a Mesozoic carbonate platform showing a slope break around km 40 (Fig. 6). Seismic reflectors of the carbonate platform have been calibrated by seismic correla-

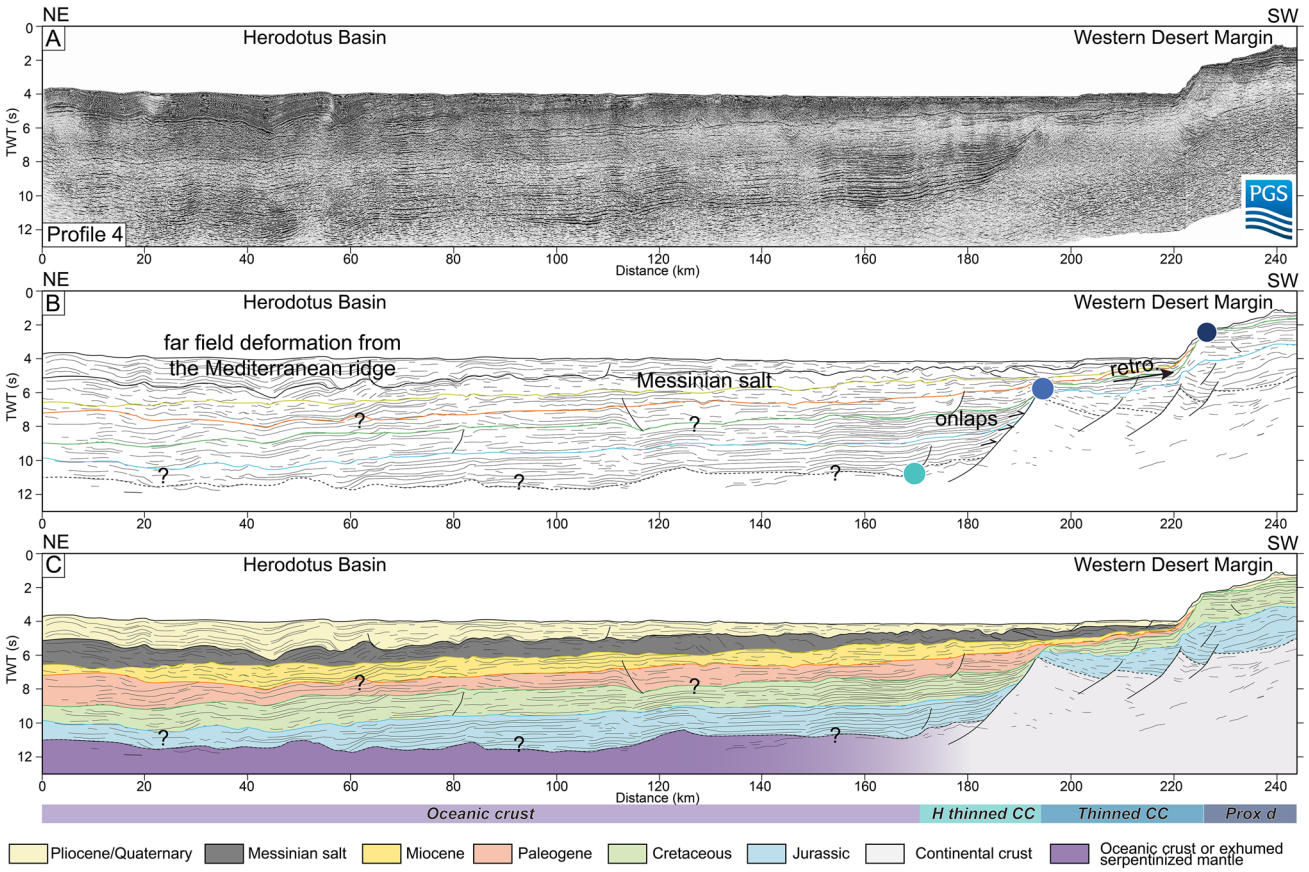

Fig. 9 **A** Un-interpreted composite seismic line D running from the Western Desert margin to the Herodotus Basin. **B** Line drawing of line D highlighting the main horizons **C** Structural interpretation of line D with the associated rift domains. Black dashed line corresponds to the interpreted top basement (Data courtesy PGS)

tion with onshore wells in the proximal domain up to latest Triassic (Bowman 2011). The thinned continental domain is characterized by NNW-SSE oriented crustal-scale normal faults below the Mesozoic carbonate platform. Our observations are in accordance with Ghalayini et al. (2018) describing growth strata controlled by NNW-SSE oriented normal faults (fault offset > 2 km) indicative of extensional activity.

The *highly thinned domain* of the northern Levant margin is confined to a narrow zone (~ 15 km) characterized by a set of major high normal faults offsetting the basement filled by pre-carbonate platform sequences (Bowman 2011). Further to the SW, seismic imaging is blurred, however thickness variations of layered sequences suggest the presence of normal faults controlling half-graben basins in the deepest part of the profile (5 s TWT) (km 25 and km 35, Fig. 6). The base of the carbonate platform is partly identifiable on seismic section. Seaward of km 40, the Jurassic and Cretaceous sequences describe a general deepening and thinning.

The *deep basin domain* is generally poorly imaged and has largely been subducted below the Latakia ridge (Fig. 5). Where it is best imaged, it is characterized by deep top basement (> 7 s TWT).

Interpretations In absence of deep drilling calibration, the timing of rift activity remains poorly constrained across both the NNE-SSW and NNW-SSE segments of the northern Levant margin. Stratigraphic correlations with onshore wells indicate that the base of the Mesozoic carbonate platform is as old as latest Triassic in the proximal domain. The interpreted presence of NNW-SSE oriented crustal-scale normal faults (Fig. 6) and growth strata (Ghalayini et al. 2018) underlying the Mesozoic platform suggest a pre-Jurassic rift phase occurred in the northern Levant margin (Fig. 6) (Bowman 2011). In the thinned continental domain, the top of the carbonate platform presents a different faulting pattern from its base (Fig. 6), suggesting that the post-rift stage began during the early development of the platform. Ages of the seismic sequences toward the deep basin are not directly calibrated. The interpretation of downlaps of carbonate debris flow on the basin basement (Bowman 2011), would suggest that the basin is younger or contemporaneous to the Mesozoic carbonate platform developed on the thinned continental margin (Fig. 6).

The crust that underlies the northernmost Levant basin is characterized by a homogeneous velocity structure (Welford et al. 2015), but the limited extent of the profile cannot be

used to unambiguously discriminate the continental or oceanic nature of the entire basin.

Multiple normal fault trends are observed at the transition from the thinned continental crust to deep basin domain in the northern Levant margin, preventing an unambiguous determination of either a normal or transform margin-type. Constraints on the timing of each set of faults are not available.

Central Levant margin

The boundary between the northern and central Levant margin segment near latitude 34° is marked by the Neogene strike slip (NNE-SSW) and compressional MLT system (Figs. 4, 5) (Carton et al. 2009; Ghalayini et al. 2018). The description of the central Levant margin structure focuses along a composite section of WNW-ESE oriented seismic lines (Fig. 7).

Delimitation and description of structural rift domains In the central Levant margin, the *proximal domain* is located eastwards, onshore (Fig. 5). Based on outcrops and the geological map of Lebanon (Dubertret 1966), the proximal domain is characterized by post-rift shallow marine carbonate of Turonian to Kimmeridgian age intercalated by fluvio-deltaic deposits.

Offshore, the *thinned continental crust domain* is characterized by the presence of the Saida-Tyr Mesozoic carbonate platform (Figs. 5, 6). At the transition between the northern and central Levant margins, the carbonate platform is absent from offshore seismic images and top basement appears to be relatively deep (> 5 s TWT), resulting in the mapping of a narrow thinned continental crust domain (near MLT, Fig. 5). NE-SW oriented normal faults with < 1 km offset (Ghalayini et al. 2018) are observed below the carbonate platform (Fig. 6). These faults sole into an acoustic basement between 5 and 7 s TWT.

The northern edge of the Saida-Tyr platform is oriented NE-SW whilst the southern edge is oriented NW–SE (Fig. 5). Both directions are partially affected by later (Cenozoic) strike slip and compressional tectonic which create a sharp (< 30 km) step between the domains of thinned continental crust and the deep basin (Nader et al. 2018). This major step in the top basement (2, 5 s TWT) is mapped as part of the domain of *highly thinned continental crust* (Fig. 7). Subsequent Cenozoic compressional deformation focused on a narrow zone above this basement step possibly reactivating a former major extensional structure (km 420, Fig. 7). On WNW-ESE oriented seismic lines (Fig. 7), the transition from the Saida-Tyr carbonate platform to the deep basin (domain of highly thinned continental crust) ranges from 5 km along the southernmost section of the central Levant margin to 30 km along the northernmost section (Figs. 5, 7). This variable width,however, does not correspond to changes in basement structure; the top basement remains planar and no clear second order structural features can be observed along the central Levant margin (Fig. 7).

The *deep offshore northern Levant Basin* (Fig. 5) is characterized by a deep smooth top basement (9 s TWT, Fig. 7) with on top of which almost planar and parallel sedimentary layers are observed until the Late Cretaceous (Fig. 6). These sedimentary layers thicken toward the North due to the influence of the Cyprus Arc/Latakia Ridge convergent system (Fig. 5).

Interpretations Reliable age constraints on rifting within this segment are scare. Within the thinned continental crust domain (Saida-Tyr Platform), Middle Jurassic (Bajocian) carbonates are deposited in a post-rift setting (Ghalayini et al. 2018) while no information from outcrop or borehole are available for older stratigraphic successions. Based on the thickness of undeformed series below a calibrated Mid-Jurassic reflector (~ 1.2 km), it seems likely that the basement faulting on the Saida-Tyr platform is as old as Triassic in age, as proposed by Nader et al. (2018).

Different interpretations have been proposed for the nature of the crust in the deep basin based on the velocity structure modeled from refraction data. Only the NW–SE oriented refraction profile of Ben-Avraham et al. (2002) (Profile I) is located north of the Carmel Fault and extends seawards at the transition between the northern and southern deep Levant basin (Fig. 5). Results of Ben-Avraham et al. (2002) showed the presence of a dense high velocity (6.5–6.7 km/s) crust, homogenenously thick, they interpreted as being oceanic crust. The E–W oriented refraction profile of Netzeband et al. (2006) (Profile P2) is located nearby and is better resolved, but its seaward part lies in the southern Levant basin. There, the crust consists of two layers with a P-wave velocity 6.0–6.4 km/s and 6.5–6.9 km/s and is interpreted as thinned continental crust (Netzeband et al. 2006). Observations from our dense seismic reflection dataset indicate, as imaged along our composite section (Fig. 7), that the top basement is consistently smooth in the northern Levant basin, without any significant perturbation indicative of faulting, in which it differs from the deep southern Levant basin.

Southern Levant margin

The southern Levant margin is located south of the Carmel Fault (Fig. 4) that has been, based on potential field data (Fig. 2), mapped offshore with a NW–SE trend and connecting with the northern boundary of Eratosthenes Seamount (Segev and Rybakov 2011; Segev et al. 2018) (Fig. 5). On seismic sections the offshore fault prolongation is not clear

and is mapped here as a change in the top basement morphology (Figs. 5, 7).

Delimitation and description of structural rift domains Seismic refraction and gravity modeling indicate minor crustal thinning onshore, grading from 33 km in thickness along the Dead Sea Fault to 28 km in thickness along the current coastline (between ca. N°33 and N°31.5) (Fig. 4, 5) (Mechie et al. 2009; Gardosh and Tannebaum 2014). This onshore *proximal domain* is characterized by kilometer-scale variations in the thickness of Late Permian to Middle Jurassic sedimentary series (Druckman et al. 1982; Garfunkel and Derin 1984) controlled by NE-SW and NNE-SSW oriented normal faults (Fig. 5).

The *thinned continental crust domain* forms a more or less 50 km wide band straddling the coastal plains and offshore basins along southern Levant margin (Fig. 5). This thinned crustal domain is covered by post-rift Mesozoic carbonate platform (Fig. 8) similar to the Saida-Tyr platform further North (Fig. 7). A few oceanward dipping faults controlling the Triassic and Jurassic extension have been mapped below these post-rift deposits (Figs. 7, 8) (Gardosh et al. 2010), some of which seems to have been reactivated upon compression (Fig. 8 km 300–310).

The *highly thinned crust domain* is narrow (~ 10 km) and is delimited eastward by the edge of the carbonate platform and westward by the deep southern Levant Basin, where the top basement is typically deeper than 8 s TWT (Figs. 5, 6, 7, 8).

South of the Carmel fault (Fig. 7), the top basement of the southern Levant basin is more rugose than the northern Levant basin and several low amplitude fold structures (20 km wide) are observed in the Cretaceous and Paleogene sequences along the *deep basin domain* of the margin (e.g. km 140, 190 Fig. 8, Saggy et al. 2018). The top basement of the southern Levant basin appears faulted contrasting with the smooth northern Levant basin. It is here distinguished from the northern Levant basin and referred to as "structured deep basin" (hatching Figs. 4, 5). Sparse, isolated, yet thick (3 s TWT), Cretaceous to potentially Jurassic carbonate platforms occur in these basins such as the 30 km wide Zhor structure (Fig. 8) which straddles the edge of the South Levant basin south of the Eratosthenes Seamount (Fig. 5).

Interpretations Evidence for extensional activity is observed in the Late Permian to Middle Jurassic sedimentary sequences (Druckman et al. 1982; Garfunkel and Derin 1984) in the onshore proximal domain. Normal faulting was associated with magmatic activity as exemplified by the onshore Asher volcanics (up to 2 km in thickness) that were emplaced in a rift basin during the Late Triassic (~ 201–206-Ma) (Asher-Atlit-1 borehole south of the CF, (Golan et al. 2021)). This magmatic activity has been related to a Late Triassic to Early Jurassic rifting leading to continental breakup (Gardosh et al. 2010).

More refraction profiles cover the southern Levant basin (Makris et al. 1983; Ben Avraham et al. 2002; Netzeband et al. 2006) and can be used together with seismic reflection observations, gravity inversion results (Steinberg et al. 2018) and magnetic anomaly maps (Segev and Rybakov 2010; Segev et al. 2018) to interpret the nature of the crust. The P-wave velocity structure of the crust (Ben-Avraham et al. 2002), the pattern of gravity (Fig. 2) and magmatic anomalies (Fig., 9A in Segev et al. 2018), differ between the northern and southern part of the Levant basin (Figs. 4, 5). Based on better resolved results in the southern Levant basin than Ben-Avraham et al. (2002), Netzeband et al. (2006) argue that their two-layer velocity model is consistent with highly thinned continental crust, the continental nature of the crust being supported by El-Sharkawy et al. (2021). Such interpretation is consistent with gravity inversion results predicting that the southern Levant basin is floored by 10 km thick crust interrupted by thicker NE-SW oriented ridges (Steinberg et al. 2018). The low amplitude folds and isolated carbonate platforms observed on seismic reflections profiles in the southern Levant basin are indeed likely to be located over pre-existing basement heterogeneities; whose structural interpretations differs depending on the authors (Tari et al. 2020; Segev and Rybakov 2011; Welford et al. 2015; Papadimitriou et al. 2018) (Figs. 7, 8). Tari et al. (2020) notably suggested that the geometry of the folds is related to the inversion of extensional half-grabens, an interpretation consistent with the predicted continental nature of the crust by refraction and gravity inversion results. It is noteworthy that several of these basement highs are associated to a strong magnetic signal, suggesting they could be intruded by magmatic rocks (Segev et al. 2018) or correspond to ancient volcanic edifices. Based on these different geophysical results, we suggest that the southern Levant basin is most likely floored by highly thinned continental crust locally intruded by magmatic additions.

Eratosthenes Seamount

The Eratosthenes Seamount is an isolated 130 km wide bathymetric high somewhat circular in shape bounded by a pronounced bathymetric trench. It is located 60 km south of Cyprus island (Figs. 4, 5). The edges of this seamount are clearly identifiable by the total horizontal gradient of the Bouguer gravity anomaly (Fig. 2B). This topographic high is bounded to the East by the southern Levant basin, to the South by the Nile Deep Sea Fan, to the West by the Herodotus Basin, and to the North by the Cyprus Arc (Figs. 4, 5).

Drill hole data in the north of the Eratosthenes Seamount from ODP Leg 160 (Ocean Drilling Project (Robertson 1998), calibrated a discontinuous stratigraphic sequence

going back to undated pre-Aptian time and includes Aptian shallow water coral limestone (ODP Site 967; Robertson 1998). In the Early Cretaceous, and maybe earlier, Eratosthenes Seamount was covered by an isolated carbonate platform surrounded by deep basins (Hawie et al. 2013). In the Late Cretaceous, the northern part of the seamount subsided (outer shelf to bathyal depth) (Robertson 1998) before being uplifted to shallower depth in the Early Miocene. The seamount recorded another important deepening event during the Late Pliocene to Early Pleistocene as a consequence of the under thrusting of the seamount and surrounding basins below the Cyprus arc during convergence (Robertson 1998).

Delimitation and description of structural rift domains

The most recent and highest resolution wide-angle seismic investigations indicate that the crust of the seamount range between 20 to 25 km thick and is most likely continental (Welford et al. 2015a; Feld et al. 2017), suggesting it can be mapped as part of a domain of *thinned continental crust* (Figs. 5, 6, 7). The transition with the Herodotus and Levant Basins is sharp and characterized by narrow domains of highly thinned crust (5–10 km) (Figs. 4, 5, 6, 7).

The seismic composites presented in the Fig. 7 provide additional information on the structure of the Eratosthenes Seamount. The interpreted top basement reflector (dashed black line in Fig. 7) is offset by several normal faults of unconstrained age (Fig. 7). In relation with these faults, one major syn-rift wedge (1.5 s TWT interval) is observed on the eastern side of the Eratosthenes seamount (between 280 and 310 km and at a depth interval between 4.7 s TWT and 6 s TWT in Fig. 7). However, the age of this syn-rift wedge is unconstrained by drilling.

Interpretation

The Eratosthenes Seamount is interpreted as an example of the Mesozoic Mediterranean type aggrading isolated carbonate platform (Rusciadelli and Shiner 2018) here over thinned continental crust (Figs. 5, 6), (Welford et al. 2015; Feld et al. 2017). Despite its variable velocity structure, the Eratosthenes Seamount hence represents a continental block detached from the Levant margin (or more generally northern Gondwana margin) during one or multiple Mesozoic extensional phase (Welford et al. 2015;). Oceanic crust is interpreted to lie west of the Eratosthenes Seamount (Longacre et al. 2007; Welford et al. 2015;) (Fig. 7).

Between the well calibration by ODP and the unambiguous top basement, an interval with a thickness of 2–3 s (TWT) is observed (Fig. 7). This interval was interpreted either as carbonate platforms (Fig. 7) (Papadimitriou et al. 2018) or as volcanic sequences (Segev et al. 2018). The age of this thick interval is not dated, but is older than Early Cretaceous, most likely Jurassic and older. The underlying syn-rift wedge observed at km 280–300 on the Fig. 7 could then be as old as Permian or Triassic (Fig. 7) as suggested by Van Simaeys et al. (2019).

Northeast Egyptian margin

The Northeast Egyptian margin is located to the south of the Eratosthenes Seamount and to the east of the southern Levant margin and represents a 500 km long E-W elongated margin between the coast of Sinai and the Nile Cone (Figs. 1, 4, 5). The tectonic evolution of this margin is poorly constrained, in part because it is covered by a thick Cenozoic clastic sedimentary succession originating from the Nile River and forming the Nile Deep Sea Fan (Figs. 4, 5, 6, 7, 8) (Loncke et al. 2006, Abdel Aal et al. 2001; Jagger et al. 2020). This margin is characterized by structures in the upper part of the sedimentary sequence linked to gravitational gliding of thick Pliocene–Quaternary clastic sediment packages (locally up to 4.5 km thick) over Messinian salt layers (up to 3 km thick) (Loncke et al. 2006) (Fig. 8) and of Miocene and Oligocene clastic sediments over Late Cretaceous/Paleogene shales. Such deformation alters the seismic imaging of the underlying strata, thereby locally hampering the identification of distinct rift domains (Fig. 8).

Delimitation and description of structural rift domains

Onshore northern Sinai, a set of NE-SW to ENE-WSW oriented rift basins have been identified (Fig. 5) (Moustafa 2010, 2020). The normal faults delimiting these rift basins have subsequently been reactivated and inverted during the post-80 Ma compressional phase (Moustafa, 2010, 2020; Moustafa and Fouda 2014) (Fig. 5). Thickness variations and age calibrations down to Early Jurassic successions suggest that the extension that generated these basins is at least as old as Early Jurassic (Moustafa 2010, 2020; Moustafa and Fouda 2014). The former half-graben basins observed onshore of the northeastern Egyptian margin are filled by Jurassic syn-extension sandstones and shales (up to 4 km thick, Moustafa 2010; Dolson et al. 2001). The continental to shallow marine depositional environments of syn-rift successions and limited extension recorded along the normal faults delimiting the rift basins is typical of rifted margin *proximal domains* recording only limited crustal thinning (Tugend et al. 2015a).

The extent of the *thinned domain* is less constrained, notably in the Nile delta area and the edge of the post-rift carbonate platform identified by Tassy et al. (2015) is used to delimit the boundary between the domains of thinned and highly thinned crust (Fig. 5).

Post-rift pre-Messinian series thicken toward the north, reaching a thickness of 7 km with a potential top basement as deep as 15 km south of Eratosthenes Seamount (Caméra et al. 2010). Crustal thickness decreases from south to north,

reaching ~ 10 km under the Nile deep sea fan (Figs. 4, 5) (Caméra et al. 2010) before increasing to ~ 20-25 km under the Eratosthenes Seamount (Welford et al. 2015; Feld et al. 2017). Normal faults with km-scale offset affecting the top basement are identified (Caméra et al. 2010; Jagger et al. 2020), but their age and orientation is difficult to resolve. Offshore North Sinai, a set of NE–SW trending normal faults, subsequently reversed to form NE-trending folds are nevertheless locally identified (Yousef et al. 2010). To the west, this *highly thinned crustal domain* is bounded by the NE-SW oriented Rosetta fault trend (Figs. 5, 8). The Rosetta trend is a Cenozoic dextral transpressive structure (Kellner et al. 2018) located over a major basement step that is well imaged by gravity and seismic data (Fig. 2).

Interpretations

The highly thinned domain is considered continental by most authors (Caméra et al. 2010; Jagger et al. 2020) based on crustal thickness estimations from depth converted seismic reflection profiles (Caméra et al. 2010) and gravity inversion (Cowie and Kusznir 2012a). The continental nature is, however, more debated toward the southern part of the Eratosthene seamount that is suggested to correspond to transitional, possibly oceanic crust (Feld et al. 2017). The Rosetta structure is inferred to be inherited from Mesozoic extension by some authors (Abd El Fattah et al. 2021). It is noteworthy that its NE-SW trend is similar to the trend of the structure delimiting the Eratosthenes Seamount further north that mark the boundary between continental and oceanic domains (Figs. 4, 5, 7) (Longacre et al. 2007). By analogy and as supported by the identification of a different lithosphere structure in the vicinity of this NE-SW trend (El Sharkawy et al. 2021), the Rosetta trend is here considered to mark the transition between the highly thinned continental crust domain and the oceanic Herodotus Basin (Figs. 4, 5).

In this passive margin segment, the calibration of thickness variations in Jurassic and notably Early Jurassic successions in onshore rift basins (northern Sinai) indicate that rifting onset is at least as old as Early Jurassic (Moustafa 2010, 2014; Moustafa and Fouda 2014), possibly Triassic (Moustafa 2020). Offshore age calibrations do not permit constraining the age of the onset of normal fault activity (Caméra et al. 2010; Jagger et al. 2020).

Western Desert margin and Herodotus Basin

The Western Desert margin runs west of the Nile Cone from the Rosetta trend to the Mediterranean Ridge (Figs. 1, 4). The Herodotus basin extends west of the Eratosthenes Seamount and Rosetta trend. The structure of the Western Desert margin and transition towards the Herodotus basin is illustrated along a NE-SWW profile (Fig. 9). Regional seismic correlations enable the calibration of Cenozoic reflectors; the exact age of the deeper sedimentary section (> 8 s TWT) remains however unknown (Fig. 9).

Delimitation and description of structural rift domains

The thinning factor map of northern Africa (Cowie and Kusznir 2012a) (SM1) predicts a 400–500 km wide domain of slightly thinned continental crust from the Egyptian coast to the Sahara metacraton. Along the Western Desert, a set of partially inverted Mesozoic extensional basins are identified (Dolson et al. 2001; Moustafa 2008, 2020). They are mostly delimited by ENE-WSW and WNW-ESE oriented high angle normal faults (Fig. 4) which control the thickening of Jurassic and Cretaceous sequences (Moustafa 2008, 2020). The presence of extensional basins and the relatively minor thinning of the crust are typical of a passive margin *proximal domain* (Fig. 5) (Tugend et al. 2015a). The proximal domain of the Western Desert margin extends offshore (Fig. 4, 5) and the youngest Cretaceous shelf edge (Tassy et al. 2015) (km 190) (Fig. 9) is used as a proxy to define the seaward boundary with the thinned domain. The persistence of a Cretaceous shallow water platform in the offshore Western Desert margin (km 190–230 Fig. 9) despite transgressive conditions (Tassy et al. 2015), suggest limited post-rift thermal subsidence (Warrlich et al. 2008), as expected in proximal domains of passive margins (Tugend et al. 2015a).

The *domain of thinned continental crust* shows well developed syn-rift fault bounded basins below the pre-Cretaceous carbonate platform (km 190–230 Fig. 9). The normal faults that we mapped within or delimiting the thinned continental crust domain are preferentially oriented in a NE-SW to WNW-ESE direction (Fig. 5). The Jurassic Matruh graben (Matruh Canyon, Fig. 5) represents an exception trending in a N–S to NNE–SSW direction (Moustafa et al. 2008, 2020; Tari et al. 2012) from the proximal to thinned continental domain (Fig. 5). A steep deepening of the top basement is observed at the boundary with the highly thinned continental crust.

The *highly thinned domain* is marked by the deepening of the top basement from 6.5 to 7 s TWT to > 10 s TWT in the deep Herodotus basin (km 178–190 Fig. 9). The transition from the highly thinned domain to the Herodotus deep basin occurs within less than 20 km (Figs. 5, 9). The deepening of the top basement is accommodated by a major normal fault as expressed on Fig. 9 or by a couple of oceanward dipping faults (Jagger et al. 2020) depending on the along strike position on the margin. The sedimentary package of the deep basin passively onlaps on these major normal faults (km 180–190 Fig. 9). The boundary between the highly thinned continental crust and the deep Herodotus basin shows on a map a well-defined linear trend-oriented WNW-ESE (Fig. 5).

In the *deep Herodotus basin*, the top basement is never clearly imaged. Based on seismic facies variation from well layered to more chaotic sequences, we suggest, in accordance with other studies (Jagger et al. 2020), that the top basement is found as deeply as 11 s TWT, on top of which ~ 7 sTWT thick undeformed sedimentary sequence were deposited (Fig. 9).

Interpretations

Onshore, in the proximal domain, a transition from continental to marine sedimentation occurs in the Middle Jurassic (Moutafa 2008, 2020). Triassic to Early Jurassic red beds within rift basins of the Western Desert show thickening toward the bounding faults (Moustafa 2020) indicating an extensional phase occurred in the Early Jurassic and the onset is possibly as old as Triassic (Moustafa 2020). The overlying Middle Jurassic marine carbonate platform is deposited in a post-rift setting (Tassy et al. 2015). Although not directly constrained by drilling, we suggest by correlations with post-rift reflectors in the proximal domain that the rift basins observed in the thinned crust domain mainly developed in the Early Jurassic. A minor younger NE-SW oriented Early Cretaceous extensional event is identified in the southern part of the proximal domain based on a fault-related sedimentary wedge (Abu Gharadig Basin Fig. 5, (Moustafa 2020)), but is proposed to be linked to the Libyan Sirte Basin extension phase further to the west (Fig. 1).

The Herodotus Basin is floored by thin crust dipping northward and westward below the over-thrusting Mediterranean Ridge (Figs. 1, 4). Interpretation of velocity data from punctual ESP (Expanding Spread Profile, Pasiphae cruise) from the Herodotus Basin suggests that a ~ 10 km thick sedimentary package overlie ~ 10 km thick crust of continental or oceanic nature (de Voogd et al. 1992). ESP velocity data from the same Pasiphae survey have recently been recalibrated against reflection seismic profiles in the nearby Ionian Basin showing that velocities of up to 4.9 km/s corresponded to old, compacted sediments deposited on top of the crust of the Ionian basin (Tugend et al. 2019). By analogies with results from the Ionian Basin, we suggest that the 4.75 km/s layer interpreted as being part of the crust by de Voogd et al.(1992), most likely corresponds to compacted sediments, in which case, the crust of the Herodotus would be ~ 8 km thick, in the range of accepted values for oceanic crust. The oceanic nature of the crust of the Herodotus basin is further supported by a recent study based on inferences from surface wave tomography and stochastic inversions suggesting an oceanic nature of the Herodotus lithosphere (El-Sharkawy et al. 2021). Based on a set of magnetic profiles Granot (2016) mapped NE-SW oriented geomagnetic inversions typical of oceanic crust in the Herodotus Basin and interpreted them as Carboniferous in age (Granot 2016). In contrast, wells penetrating Paleozoic successions and seismic sections from the Western Desert and Levant margins have shown no compelling evidence for such an extensional event in the Carboniferous (Frizon De Lamotte et al. 2015).

Based on the age of faulting activity in the proximal domain (Moutafa 2008, 2020) and the age of the shift to post-rift passive carbonate platform building on the Western Desert margin (Tassy et al. 2015) we suggest breakup occurred sometime in the Early to Middle Jurassic and was followed by oceanic spreading in the Herodotus basin.

Identifying rift and spreading events in the Eastern Mediterranean Sea: integration of the onshore geological record

The EMS is located at the western tip of the Tethys embayment from Late Paleozoic to mid Cretaceous (Şengör and Yilmaz 1981) following the Carboniferous assemblage of the super-continent Pangea (Matte 2001). The Mesozoic paleogeographic evolution of the EMS is characterized by a complex spatial and temporal succession of extensional events, associated with the opening of oceanic basins, and compressional events associated with subduction, obduction and collision. As a result, the Tethys domain found between Gondwana (Greater Adria, Africa, Arabia, Fig. 10) to the South and Eurasia to the North, present multiple Mesozoic oceanic basins (Meliata, Küre, Malliac, EMS, Balkan Neo-Tethys, Pindos) separated by continental block (Pelagonia, Tripoliza, Taurus, Dacia, Circum Rhodope, Apulia), whose timing, basement nature, geodynamic origins and paleogeographic positions remain highly debated (Fig. 10) (Stampfli and Borel 2002; Robertson and Mountrakis 2006; van Hinsbergen et al. 2020).

The EMS has been the focus of extensive sedimentary, structural, geochronological, petrological, geophysical studies conducted over more than a century (e.g. Laubscher and Bernoulli 1977; van Hinsbergen et al. 2020)) and a comprehensive review of all the tectonic events that affected the EMS is beyond the scope of this contribution. In the following section we focus on the geological evidence for rifting and continental breakup that affected the EMS and direct surroundings. We combine our offshore observations with a detailed review of onshore rifting evidence from the northern and western side of the EMS. We have benefited from recent tectonic maps from the Eastern Alps to Western Turkey and paleographic reconstructions from Schmid et al. (2020) and Van Hinsbergen et al. (2020) respectively (SM2) that homogenized the different tectonic and paleographic domains across the EMS. On this tectonic map, we show the evidence for rift events based on the stratigraphic record (such as facies changes from shallow to deep marine conditions) and tectonic activity on the corresponding paleogeographic domain (hexagon SM2). On that map (SM2) we also

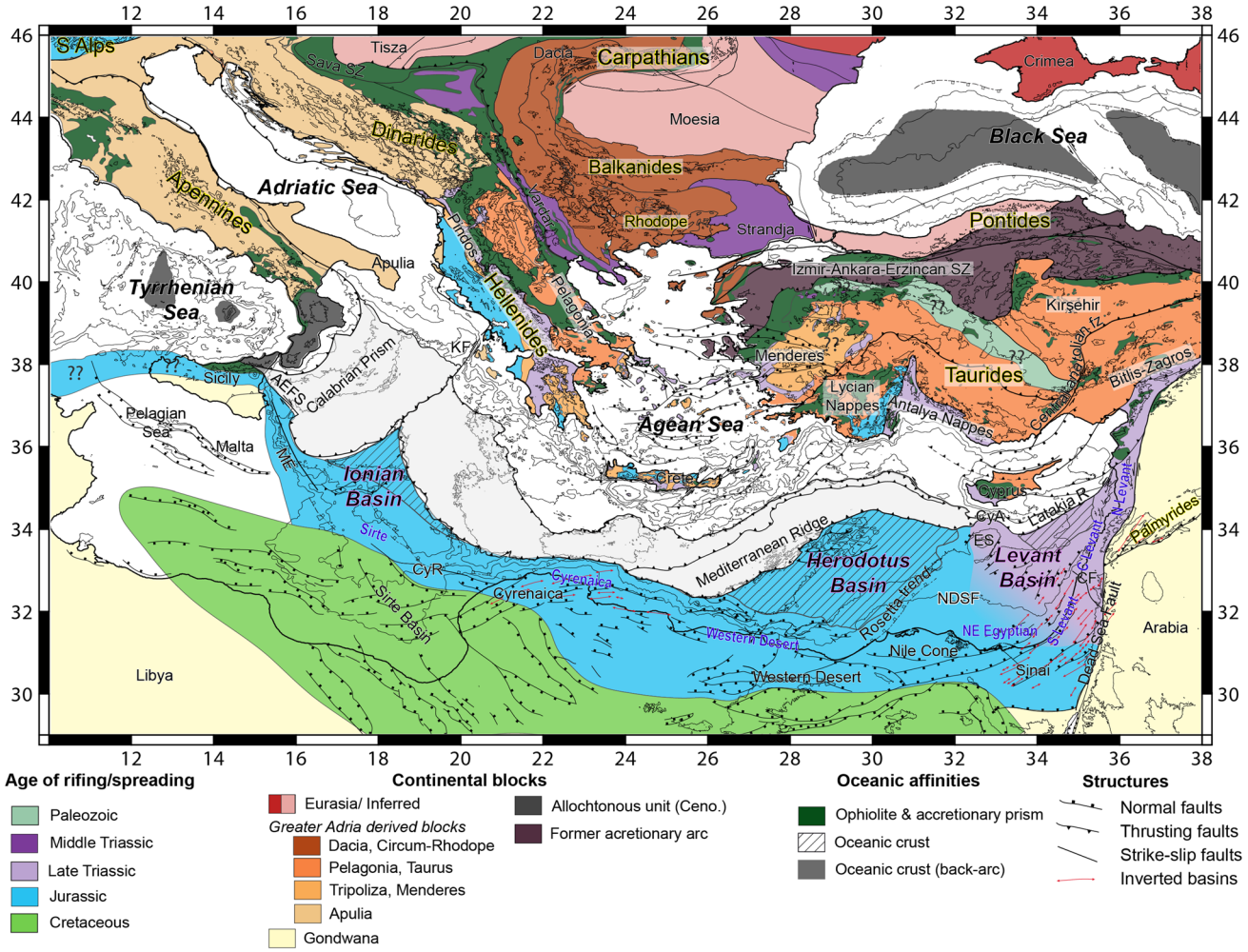

Fig. 10 Map of the EMS showing the age of the main rift or spreading events affecting the different domains (modified from the tectonic maps of Schmid et al. 2020; Van Hinsbergen et al. 2020). See supplementary material 2 **(SM2)** for the geological evidence integrated in this interpreted map

plot, when available, the age of the youngest pre-Mesozoic metamorphic event that affected the basement rocks (squares SM2), providing information of pre-rift paleo-geographical affinities. We also illustrate the age of ophiolite obduction and of the oldest compressional structures (circles SM2). This compilation is the backbone of our interpreted rift event map (Fig. 10), which highlight the location and age of extensional activity in between continental micro-blocks.

Permian

The northern part of the EMS (N Adria, Rhodope (Balkans), Pontides (Turkey)) (Fig. 10) was affected by the Carboniferous Variscan orogeny, with metasedimentary greenschist low grade metamorphism (Sibila Borojević et al. 2012) and un-metamorphosed Carboniferous silicoclastic series (flysch) related to convergence (Spahic et al. 2018). Following Variscan compression, Permian post-orogenic extensional and trans-tensional events are observed in Western, Central Europe and NW Africa (Arthaud and Matte 1977). Around the EMS, evidence for extensional basins possibly related to this event are observed in Central Sicily (Imerse and Sicanian Basin, Basilone et al. 2016), Puglia (Lagonegro Basin, Ciarapica and Passeri 2002), Crete, Peloponese, Evia (Phyllite Quartzite Unit, Robertson et al. 2006) (SM2) and characterized by Permian (even Carboniferous in Crete) deep-water sedimentary facies (paleo bathymetry > 500 m). In these areas, evidence for an extensional event is only based on lateral facies variation. No clear fault structures of Permian age have yet been identified. Stampfli and Kozur (2006) interpret these basins as a Permian passive margin linked to the separation of the Cimerian block and the opening of the Neo-Tethys. This interpretation correlates with the opening of the Central Neo-Tethys further to the East between Oman (Gondwana) and Iran (Cimerian block). However, this correlation remains debated as Permian deep-water sediments

are located over domains that show only moderately thinned continental crust and no direct relation between these sediments and ophiolites are observed in the EMS. Therefore, we favor an interpretation linking the formation of these basins to a Permian trans-tensional setting (Robertson et al. 2006), which explains the architecture and sedimentary sequences of these basins.

Evidence for Permian rifting in regions unaffected by the Variscan orogeny is documented in the Palmyrides thrust and fold belt (Syria) (Fig. 1). This belt results from the reactivation of former Late Permian to early Middle Triassic ENE-WSW oriented rift basins (Brew et al. 2001). These rift basins were characterized by clastic sedimentation (alluvial plain with periodic marine influence, Barrier et al. 2014) sealed by the Middle to Late Triassic Kurachine formation composed of dolomite and evaporites. These syn- to post-rift continental to shallow marine sediments are 2 km thick at the main depocenter, indicating limited post-rift subsidence and weak crustal thinning (Brew et al. 2001). Although Permian syn-sedimentary faulting is not observed along the southern Levant margin, the depositional geometry, the sedimentary thickness and the erosional surfaces suggest a similar extensional episode as in the Palmyrides (Al Saad et al. 1992; Garfunkel 1998).

Middle Triassic

Several tectonic units from the Eastern Alps, Dinarides, Hellenides, preserving the remnants of the northern margin of Gondwana (i.e. Greater Adria promontory), show evidence of a Middle Triassic rifting associated with the opening of the Balkan Neo-Tethys ocean separating Dacia-Circum Rhodope from Greater Adria (Schmid et al. 2020; Van Hinsbergen et al. 2020; Fig. 10).

In the Alps (Fig. 10), the Hallstatt pelagic limestones are interpreted to be deposited in the distal Adriatic rifted margin after Middle Triassic breakup of the Balkan Neo-Tethys system (Gawlick et al. 2016). Further to the southeast, in the Dinarides (Fig. 10), the Middle Triassic transition of shallow marine to hemipelagic carbonates associated with local volcanism and radiolaria deposits are related to a similar rifting event culminating in the opening of the Meliata Ocean (one branch of the Balkan Neo-Tethys Ocean) (Missoni et al. 2012; Sudar et al. 2013). In the Hellenides, previous studies (Ferriere et al. 2016) recognized the elements of a former proximal to distal margin of the Neo-Tethys in the eastern part of Pelagonia (still part of Great Adria) (Fig. 10). Pre Middle Triassic sediments represent a pre-rift shallow water facies, which transitions into a Middle Triassic series with a pelagic facies, indicating a depositional environment over the distal margin during the rifting and spreading of the Balkan Neo-Tethys (Ferriere et al. 2016). This data emphasized the opening of an oceanic domain, the Balkan Neo-Tethys, during the Middle Triassic. However, evidence of Middle Triassic rifting and oceanic opening is limited to the Balkan Peninsula (e.g. Alps, Dinarides, Hellenides) (dark purple, Fig. 10).

Late Triassic

Evidence for Late Triassic extension is recorded in tectonic units all along the northern rim of the EMS from Albania to SE Turkey (light purple Fig. 10). Most of these tectonic units, preserved in nappes stacks, encompass large tectonic movements during Mesozoic to Cenozoic compressional phases, complicating their geological interpretations (Van Hinsbergen et al. 2020).

In Greece (Pindos area, Fig. 1), the stratigraphic evolution (Auboin 1959; Fleury 1980) is characterized by the transition from Middle Triassic clastic sediments overlain by Late Triassic pelagic Halobia limestones associated with chert beds and volcano-clastic deposits (Ozsvàrt et al. 2019). Jurassic and Early Cretaceous sedimentation alternates between more carbonaceous and more siliceous pelagic sedimentation until the deposition of Cenomanian–Turonian flysch-type series indicating the onset of a regional compressional regime (Auboin 1959). This stratigraphic sequence recorded the separation of the Pelagonia block from Greater Adria leading to the opening of the Pindos basin, whose exact size and nature remains debated. Late Triassic deep marine environment (Halobia limestones) associated with Cretaceous ophiolitic series are observed from southern Turkey (Moix et al. 2013) to the Mamonia unit (S Cyprus) (Robertson and Shallo 2000), indicates a similar stratigraphic evolution along the northern sections of the EMS at that time (Pindos-Turkey-Cyprus) (Fig. 10). In Syria, the Late Triassic to Cretaceous Baër-Bassit mélange found below a Cretaceous ophiolitic nappe (Figs. 5, 6, 7, 8, 9 and 10) is interpreted as the sedimentary sequence of the NE Arabian distal margin. This sedimentary sequence together with the Baër-Bassit ophiolite was thrust over Arabia in the Late Cretaceous (Al-Riyami and Robertson 2002). Taken together, these Late Triassic units are interpreted as the Eastern prolongation of the Pindos basin marking the separation between Taurus (lateral equivalent of Pelagonia) and Gondwana (i.e. Arabia) (Fig. 10).

A southeastward prolongation of this Late Triassic rifting phase is suggested in the northern and central Levant margin based on seismic and borehole observations (Fig. 10 e.g., Ghalayini et al. 2018 and Sect. 4). Towards the south, Triassic extensional faulting with kilometric offset associated with syn-rift sequences is described in the southern Levant margin (Israel, Sinai and Jordan) (Garfunkel and Derin 1984) (Fig. 7). This Late Triassic rifting phase is followed by an Early Jurassic rifting event characterized by thicker depocenters (Druckmann 1974). This poly-phased evolution

suggests that continental breakup was not achieved in the Triassic in the southern Levant Basin.

Jurassic

Observations of Early Jurassic rifting events are widespread around the EMS from Apulia to the Northwest, Africa to the South and Arabia to the East (in blue Fig. 10). Dredges collected along the Malta Escarpment (Bizon et al. 1985) and well observations on the Apulian platform (see compilation in Tugend et al. 2019) (west of the Ionian Sea, Fig. 10) highlight a late Early Jurassic deepening of the paleo-bathymetries with intercalated basalts and volcano-clastic sequences (Biju-Duval et al. 1983). The correlation and calibration of these sequences towards the deep Ionian Basin enabled Tugend et al. (2019) to constrain the age of the basin to the late Early to Middle Jurassic, despite the lack of high-resolution geophysical data. A series of inverted tilted fault blocks and associated growth strata has previously been identified along the eastern Cyrenaica margin (Fig. 10; Arsenikos 2014; Tugend et al. 2019). Well data calibrations enabled to determine that syn-rift deposition occurred prior to the late Middle Jurassic but the onset of subsidence remains unconstrained (Arsenikos 2014; Tugend et al. 2019; Jagger et al. 2020). Onshore, in the Western Desert, Early Jurassic clastic sediments are deposited on a Paleozoic erosional surface, marking the onset of subsidence and rifting (Dolson et al. 2001). This extensional phase persisted until the Middle Jurassic and created syn-rift grabens filled predominantly by clastic sediments (> 2.5 km thick, Dolson et al. 2001). Offshore, on the Western Desert margin, the Cretaceous/Late Jurassic carbonate platform morphology is interpreted as a typical post rift passive margin carbonaceous sedimentary sequence (Tassy et al. 2015). Below this sequence, we observed undated extensional faulting and interpreted them as the result of Early to Middle Jurassic rifting which led to the formation of the oceanic Herodotus Basin.

Onshore of the southern Levant margin, seismic sections have imaged half-graben geometries, which, on the basis of well calibration, indicate a series of Permian to early Middle Jurassic pulsated rifting events (Garfunkel 1998). Strong rift subsidence (> 2 km) during Early Jurassic to early Middle Jurassic associated with volcanic activity is recorded. After this rifting event, sedimentation is dominated by a shallow water carbonate platform facies. A similar tectonic setting is proposed offshore of the southern Levant Basin (Gardosh et al. 2008) including an Early Jurassic phase of extreme crustal thinning associated with magmatic intrusions (Steinberg et al. 2018).

Along the northern sections of the EMS, the Mesozoic stratigraphy of the Ionian zone (highlighted in light blue: Albania, western part of Greece, Crete and Rhodes, SM2) records a drowning event leading to the deposition of Middle Jurassic to Cretaceous pelagic and hemipelagic series (Robertson and Shallo 2000). The Ionian zone (in blue SM2) underthrust the Gavrovo-Tripoliza unit (Fig. 10 SM2) which shows only Mesozoic shallow carbonate platform facies. Within the composite Lycian nappes in southwestern Turkey, the Tavas nappe presents a similar Middle Jurassic drowning event, suggesting a connection with the Ionian zone (Fig. 10 SM2) (Poisson 1984). Taken together, the geological record both onshore and offshore on the greater Adria and on the northern Africa margins favors an Early to early Middle Jurassic rifting and spreading phase that affected most of the preserved EMS. At larger scale, this Early to Middle Jurassic period corresponds to the main rifting phase recorded in the Alpine Tethys domain to the west (Lemoine et al. 1986; Mohn et al. 2010).

Cretaceous

Evidence for rifting is found in the onshore/offshore Sirte Basin (northeastern Libya Fig. 10) were Early and Late Cretaceous syn-rift packages have been identified (Abadi et al. 2008; Jagger et al. 2020). Onshore along the Western Desert, a Cretaceous reactivation of extensional faults is observed with a clear sedimentary thickening on structures oriented in NW–SE to WNW-ESE (Moustafa 2020) (Fig. 10). This Northeast African rifted basin never reached the breakup stage. Multiple ocean island basalts are disseminated on the Southern and Central Levant Margin and show different Cretaceous ages (See the compilation of Segev et al. 2018). This magmatism has been related to possible Cretaceous back-arc extension limited to the Levant Basin (Segev et al. 2018).

Discussion

Tectonic evolution of the EMS rifted margins

By compiling the interpretation of seismic sections, gravity anomaly maps, borehole data and stratigraphic records of former conjugate margins preserved in orogenic belts, we illustrate the structure and rift evolution of the EMS margins along the northern and southern Levant Basin and the Herodotus Basin.

Inheritance

Compositional, structural or thermal inheritance of the lithosphere prior to extension are key parameters influencing the modes and locations of rifting and breakup (Petersen and Schiffer 2016; Sapin et al. 2021). Seismic reflection images on the EMS margins are not accurate enough to determine the internal structures of continental lithosphere rifted during the Mesozoic. We note, however, that the rift events do

not affect the cratonic area (SM1) and are rather localized within thinner Cadomian crust on the northern margin of Gondwana (Cowie and Kusznir 2012a; Sobh et al. 2019See thinning factor map SM1). Based on outcrops on the northern side of the EMS, borehole data and crustal thinning map (SM1), this Cadomian continental crust is characterized by granitoids intruding metasedimentary nappe stacks (Avigad et al. 2016). This continental lithosphere is suggested to form at an active convergent plate boundary during late Neoproterozoic and Early Paleozoic, somehow similar to present-day Western Pacific accretionary systems (Garfunkel 2015). A similar inherited lithosphere is present on the South China Sea rifted margins (Savva et al. 2014; Ye et al. 2018), where it has been shown that crustal structures and thermal regime contributes significantly to the deformation style and on the localization of extensional structures.

Northern Levant Basin

The evolution of the northern Levant Basin extensional activity is shown on section A of Fig. 11. Rifting activity began in the Late Permian to Middle Triassic. It is well

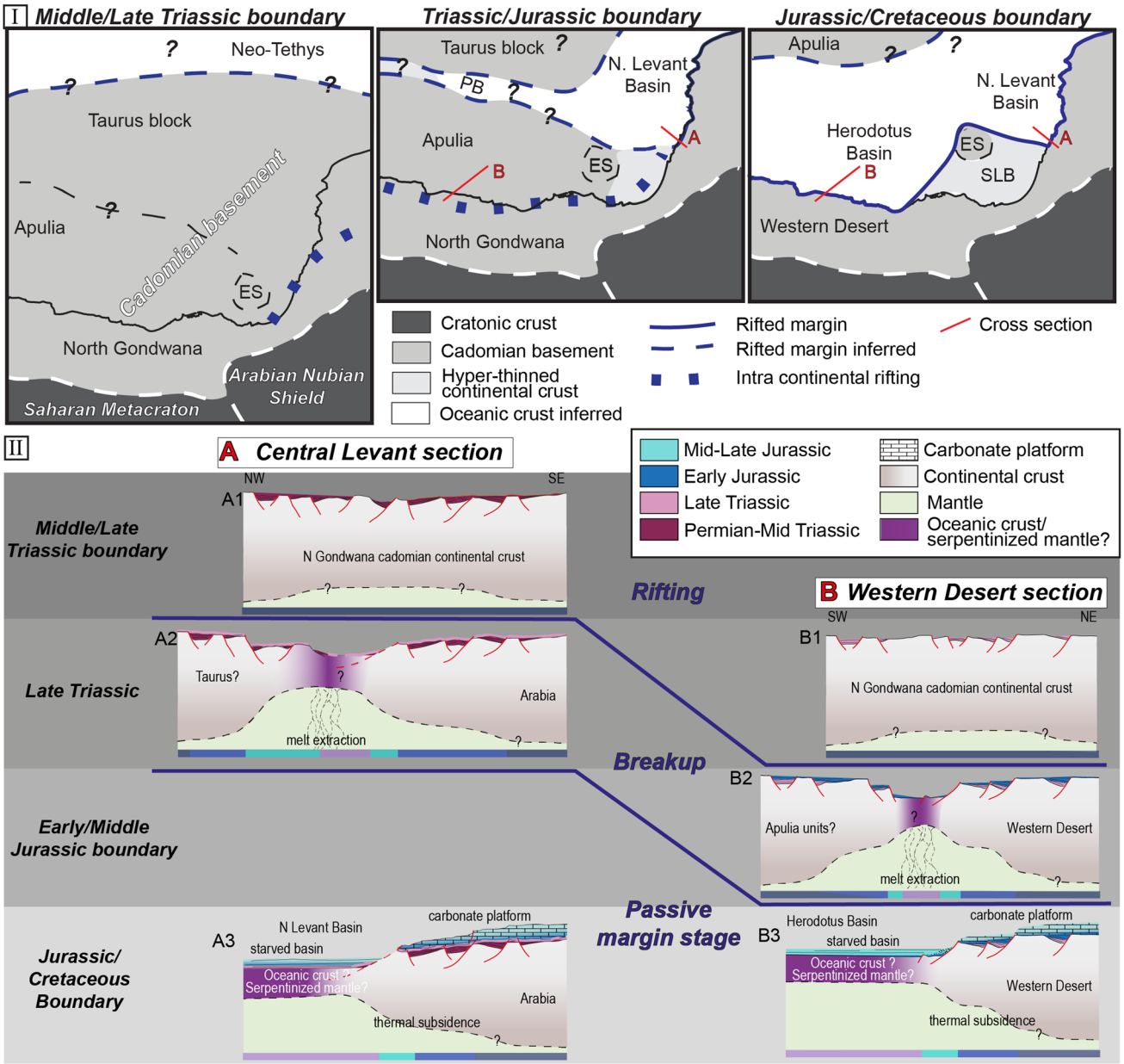

Fig. 11 Rift domain map associated with evolutionary schematic cross section of the central Levant (**A**) and Western Desert (**B**) margins. B: Basin; CF: Carmel Fault; ES: Eratosthenes Seamount

recorded in the Palmyrides (Fig. 1) and affects the central and northern Levant margin segments with a ENE-WSW trend (Ghalayini et al. 2018) (Figs. 5, 6, 7, 8, 9, 10, 11 A1). Initial rift basins are filled by clastic sedimentation followed by evaporitic formations and shallow marine carbonates indicating an intra-continental rift episode with limited crustal thinning (Al-Saad et al. 1992; Best et al. 1993; Garfunkel 1998). On the northern and central Levant margins thinned continental crust domain, the post-rift stratigraphy is calibrated down to the Middle Jurassic (Bowman 2011; Ghalayini et al. 2018) (Figs. 4, 5). The interval between the Middle Jurassic calibrated reflector and the base post-rift horizon, sealing normal faults, reaches locally more than 1 km in thickness (Ghalayini et al. 2018; Nader et al. 2018; Van Simaeys et al. 2019) (Fig. 11A2), suggesting that rifting around the northern Levant basin was older. The narrow, highly thinned domain (< 20 km) is expressed by one major normal fault associated with the necking of the continental crust (Fig. 11A2). The strong tapering of the continental crust (Fig. 11A2) is likely to generate magmatism by decompression melting (McKenzie 1984) and could result in the formation of igneous crust. Our seismic observations of the deep basin of the northern Levant basin consistently shows a horizontal top basement without structural highs. Observations from hyper-extended magma-poor rifted margins show that a rough top basement topography is typically associated with upper crustal faulting (Whitmarsh et al. 2001; Reston 2009). A smooth top basement could, in theory, be related to extension of continental crust, but this would require the entire ductile deformation of continental crust. This is not compatible with the observed steep and localized normal faults on the adjacent central Levant margin and Eratosthenes Seamount (Fig. 7). Based on these observations, we think it is unlikely that the northern Levant basin is floored by thinned continental crust. Instead, we suggest that this deep basin might be floored by oceanic crust or a magma-poor ocean continent transition (OCT), both being characterized by relatively smooth basement morphologies. Following continental breakup, the basin is characterized by a starved sedimentation as observed on the Mamonia and Baer Basit units (Al-Riyami and Robertson 2002; Torley and Robertson 2018) and the development of a carbonate platform on the margins during the Mesozoic (Fig. 11A3).

Based on offshore datasets alone, the breakup age is not constrained along the northern Levant basin. However, onshore geological data integrated in nearby fold and thrust belt can provide additional constraints. The Mesozoic Baër-Bassit mélange below the ophiolite (Syria Fig. 5) and the Mamonia unit (Cyprus Fig. 5) are located within the Cyprus Arc convergent system north of the northern Levant basin. These units contain Late Triassic pelagic Halobia limestones overlain by Early Jurassic radiolarites, implying a Late Triassic position at the base of the continental slope (Robertson et al. 2007). The Baër-Bassit mélange was scraped off during the Cretaceous supra-subduction obduction and thrusted over Arabia in a SE direction (Al-Riyami and Robertson 2002) indicating that this unit could correspond to a slice of the northern Levant margin. Based on the Triassic-Jurassic facies evolution, we infer that breakup was achieved by Late Triassic in the northern Levant basin (Fig. 11A2). Late Triassic pelagic facies are observed westward in the Pindos extensional system in Cyprus, southern Turkey and Greece (Ozsvárt et al. 2019) (SM2), which separates northern Gondwana from Pelagonia and Taurus. The exact size and nature of the Pindos is debated (Channell and Kozur 1997; Stampfli and Borel 2002; Schmid et al. 2020). Based on these arguments however, we suggest that this oceanic basin pinched out westward and transitioned into a hyper-extended continental basin.

Herodotus Basin

The evolution of the Herodotus rifting is presented on section B of Fig. 11. In the Western Desert proximal domain (Fig. 11B1), Late Triassic clastic sediments are separated from the underlying Paleozoic substratum by a major unconformity (Moustafa 2020). These Late Triassic sediments were deposited within a half-graben structure, suggesting an onset of continental extension during Late Triassic (Dolson et al. 2001; Moustafa 2020). Continuous extension during Early Jurassic creates rift basins of more than 1 km in thickness (Moustafa 2008, 2020). Along the Western Desert margin, the thinned continental crust domain is narrow and characterized by a few large offset normal faults Figs. 9, 11B2). Based on seismic interpretations and well correlation, the post-rift stage is reached at the latest in the Bajocian (Middle Jurassic) (Tassy et al. 2015) (Fig. 11B2). A similar morphology to that of the northern Levant basin margin is observed, characterized by a sharp transition from thinned continental crust to the deep basin occurring within less than 20 km (Fig. 11B2). The conjugate margin of the Western Desert margin is sampled in the Ionian zone and Gavrovo-Tripoliza platform (Dercourt et al. 1993; Frizon de Lamotte et al. 2011) (Figs. 10, 11, SM2) showing a late Early-Middle Jurassic drowning event (Robertson and Shallo 2000) consistent with a breakup at that time. The Herodotus basin, similarly to the Ionian basin (Tugend et al. 2019), is most likely the result of the separation of the southern margin of greater Adria from northern Africa.

Southern Levant Basin

The southern Levant basin is located at the SE corner of the EMS at the junction between the Herodotus and Northern Levant Basin. In the proximal southern Levant margin (Israel, Fig. 5), Permian sedimentary sequences do not show

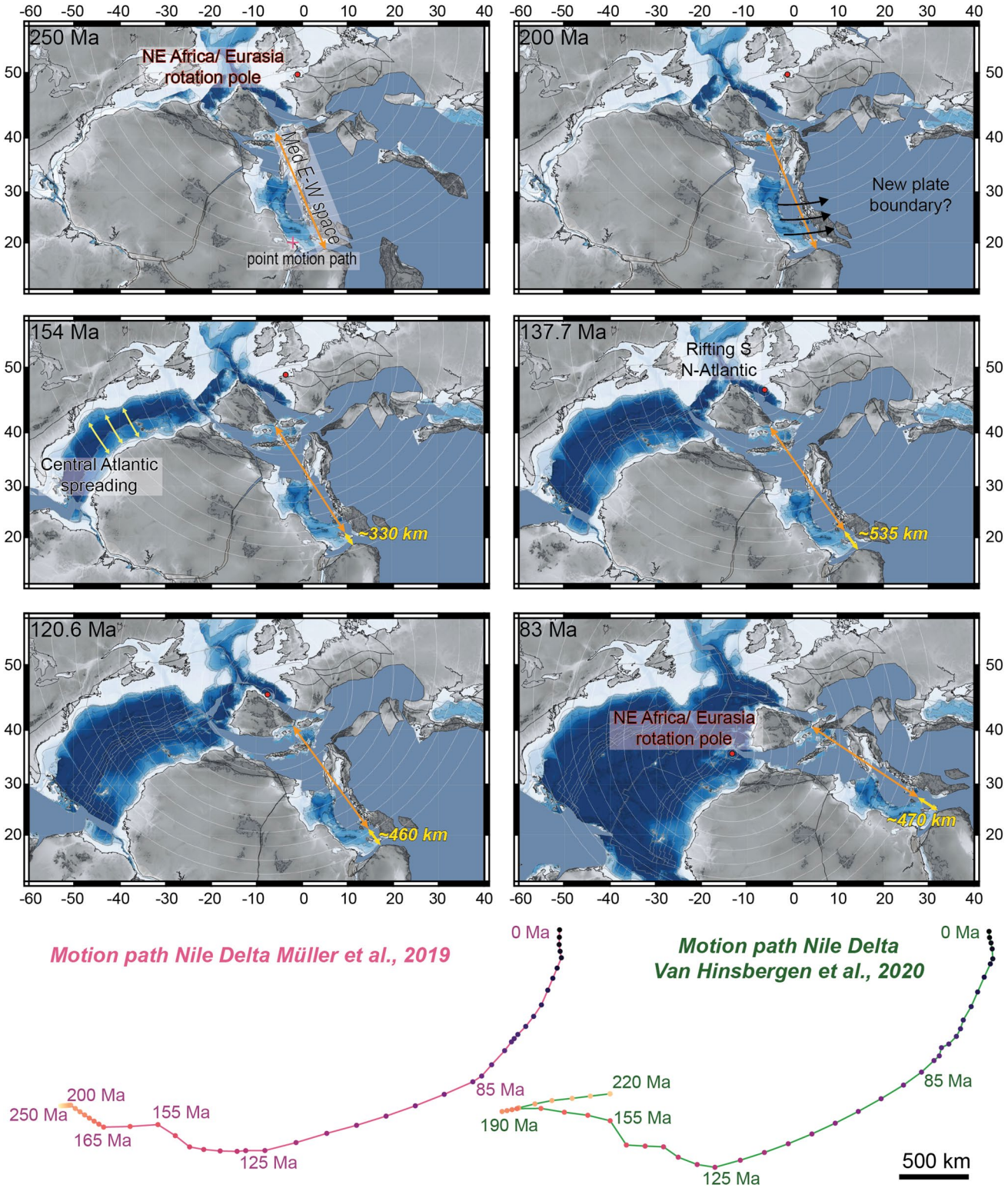

syn-sedimentary faulting (Garfunkel 1998). However, the thickness of these sedimentary deposits vary significantly, reaching locally 500 m in thickness, suggesting an intra-continental rift episode associated with the Palmyrides extension (Al-Saad et al. 1992; Best et al. 1993; Garfunkel 1998). This is consistent with kilometric offsets of middle Triassic to latest Triassic faulting along the southern Levant shoreline (Fig. 5). Onshore extension stopped at the end of the Triassic and is marked by an unconformity at the base of the Early Jurassic beds (Garfunkel and Derin 1984; Golan et al. 2021).

◂**Fig. 12** Plate reconstruction from the Permian–Triassic boundary to the end of the Cretaceous Magnetic Quiet Period (C34, ~ 83 Ma) of the Mediterranean area and surroundings (Müller et al. 2019). The micro-plate motions between Iberia (fixed to Eurasian up to Cretaceous) and Arabia are from Müller et al. (2019). Red dots indicate the position of the rotation pole of NE Africa relative to fixe Eurasia, the white circles are the associated small circles. We evaluate the maximum extension in the Mediterranean area at different age in a direction collinear to the northern Africa margin (orange arrows). At the bottom of the figure, the motion paths of NE Africa relative to fixed Eurasia from plate models of Müller et al. (2019) and Van Hinsbergen et al. (2020) are plotted to illustrate the differences in the proposed Triassic and Jurassic evolution of the system. The red cross on the upper left panel indicates the position of the point used to create the two motion paths

Renewed extension superimposed on those structures occurs in the Early Jurassic up to the Middle Jurassic (Bajocian), leading to the deposition of ~ 2 km thick sedimentary layers associated with volcanic rocks (Garfunkel 1998). Such evolution would be in agreement with a migration of extensional deformation from the Late Triassic to Early Jurassic from the proximal to the distal domains as documented in many rifted margins (Ranero and Pérez-Gussinyé 2010; Masini et al. 2011). An alternative model suggested a Cretaceous opening of the southern Levant associated with plume magmatism and back-arc extension (Segev et al. 2018). However, such a model fails to explain the pre-Cretaceous subsidence, tectonic and magmatic evolution (Golan et al. 2021). The domain of highly thinned continental crust is affected by a complex and wide area of deformation, contrasting with the sharp crustal necking we documented along the Herodotus and northern Levant systems (Figs. 4, 5). Most of the basement highs below the Nile Deep Sea Fan and in southern Levant Basin are located below folds (Figs. 7, 8). The basement highs have elongated irregular shapes in map view (Fig. 5). These shapes have been interpreted as volcanoes (Gardosh and Druckman 2006), differential growth of carbonate build up (Roberts and Peace 2007) and/or former tilted blocks (Tari et al. 2020). Following the gravity modeling of Steinberg et al. (2018), this domain could be floored by highly thinned continental crust with local magmatic additions. To the North, the gradual transition from a rough to a smooth top basement defines the boundary between southern and northern Levant basins. To the West, the transition toward the Herodotus basin is marked by a basement step along the Rosetta trend amplified by a Cretaceous to early Cenozoic folded structure (Figs. 4, 5, 6, 7, 8). We suggest that this domain is floored by highly thinned continental crust resulting from poly-directional extensional events during Permian to Middle Triassic, Late Triassic and finally Early- to Middle Jurassic (Gardosh et al. 2010). We suggest that the southern Levant Basin was first extended during the propagation of the Pindos branch in the Late Triassic and subsequently re-extended in a different direction during Early Jurassic Herodotus rifting and spreading onset (Fig. 11). An Early Jurassic age for the opening of the Herodotus basin would make its formation synchronous to the Ionian Basin (Tugend et al. 2019).

Potential kinematic driving forces and implication for plate modeling

The synthesis of rift events in the EMS (Fig. 10) reveals a southwestward younging trend of rifting age and breakup (Fig. 10). The Middle Triassic breakup is restricted to the Balkan Peninsula opening the Balkan Neo-Tethys (van Hinsbergen et al. 2020). The late Triassic rift episode runs from the Bitlis Zagros thrust to the Pindos basin (Greece) and branches with the northern Levant basin to the southeast (Figs. 1, 2, 3, 4, 5, 6, 7, 8, 9, 10). The Early to Middle Jurassic extension leading to oceanic spreading focused on the Herodotus and Ionian basins. Finally, Cretaceous rifting affects North Africa from the Sirte Basin to the Red Sea coast (Moustafa 2020) (Fig. 10). Between these basins of different ages, elongated un-thinned continental ribbons covered by Mesozoic carbonate platforms formerly part of northern Gondwana (Greater Adria promontory) are observed (Gavrovo-Tripoliza, Pelagonia, Taurus Fig. 10). Continental breakup during these rift episodes seems to be located at the northern margin of Gondwana and seems to be followed by transient seafloor spreading. This pattern, initially characterized by Sengor et al. (1984) as Tethyan dynamic, stops to the west of Apulia with the Middle-Late Jurassic Ligurian Tethys opening (Fig. 10) in a Central Atlantic dynamic (Lemoine 1983).

A critical limitation for detailed plate reconstructions in the EMS during the Mesozoic is the absence of kinematic markers, such as transform faults or unambiguous oceanic magnetic anomalies. Moreover, the sharp necking of EMS margins (Western Desert margin, central Levant margin) hampers the identification of orthogonal or transform passive margin segments. However, in between Eurasia to the North and Gondwana to the South (Fig. 12) the EMS is located in the NW termination of the Tethys Ocean. Hence, the relative motion between those two continents (represented by the small circles, Fig. 12) control the available space in the EMS domain. Based on Müller et al. (2019), the available space has been constantly shrinking since 250 Ma. From 250 to 120 Ma this space shrank at relatively slow rate prior to accelerating after 120 Ma due to the northward motion of Africa (SM3).

The geodynamic drivers controlling rifting in the EMS are controversial (Şengör and Yilmaz 1981; Stampfli and Borel 2002; Frizon de Lamotte et al. 2011; van Hinsbergen et al. 2020). Le Pichon et al. (2019) interpret the EMS as a mega pull-apart basin controlled by the spreading of the Central Atlantic and resulting from the relative motion

between Eurasia, Adria and Africa before 120 Ma. In this interpretation, the Northeast African margin, including the Western Desert margin, is a transform segment. This proposition implies a ~ 50° clockwise rotation of Adria/Apulia relative to Africa, which is inconsistent with paleomagnetic data (Muttoni et al. 2013). This interpretation is also inconsistent with the current plate circuit, as it would imply Jurassic compression in the northwestern boundary of Apulia where the Ligurian Tethys rifting developed at that time (Mohn et al. 2010).

Van Hinsbergen et al. (2020) proposed a Carboniferous Herodotus oceanic basin following Granot, (2016) and an opening of the EMS during the Late Triassic to Early Jurassic in a direction parallel to the Levant margin (green motion path from 220 to 180 Ma Fig. 12). However, this extension, resulting from the relative motion between Africa and Eurasia, would create an overlap of > 200 km in the Bay of Biscay at 220 Ma which cannot be resolved by continental rifting in palinspatic restorations (Nirrengarten et al. 2018; King et al. 2021).

Based on the global plate model of Müller et al. (2019), we test the amount of extension expected in the whole Mediterranean domain from eastern Iberia to the Levant margin (Fig. 12, Position between Iberia and Arabia are not constrained by kinematic data and are debated; here we aim to focus on the major plate motions). Assuming the continental full fit and the early seafloor-spreading of the Central Atlantic are valid, this test quantifies the maximum amount of extension accommodated in the EMS in a direction parallel to the northern African margin (Fig. 12). This results in a maximum of ~ 535 km of extension between 250 and 137.7 Ma (Fig. 12) which results from the strike slip corridor joining the Tethys subduction below Eurasia and the Central Atlantic opening (Keppie 2015). However, this distance is insufficient to explain the > 1000 km elongated (E–W in present-day coordinates) EMS along the northern Africa margin. This amount of extension implies that the different basins forming the EMS could not have opened in the same direction (E-W in present-day coordinates) only as a result of the Central Atlantic spreading. It is necessary to add an extensional component oblique or orthogonal to the northeastern African margin (N–S in present-day coordinates) to create the EMS. As space between Eurasia and Gondwana was shrinking throughout the Mesozoic (**SM3**), the EMS extension could partly have been accommodated by active convergent plate boundaries to the south of Eurasia. The position, orientation, number and evolution of convergent plate boundaries south of Eurasia from Late Triassic to Cretaceous cannot be unequivocally interpreted by geological data. However, subduction zones are suggested in most of paleogeographic studies (Şengör et al. 1984; Stampfli and Kozur 2006; van Hinsbergen et al. 2020) to accommodate the ongoing spreading of the Neo-Tethys spreading without gain of space between Eurasia and Gondwana (SM3). The Tethyan subduction dynamic and Central Atlantic opening are two competing geodynamic engines that probably lead to poly-phased rifting and transient spreading systems with multiple ridge reorganizations. Future onshore studies to locate the Triassic-Jurassic subduction zones and offshore studies to determine the opening kinematic of the Central Atlantic prior to the unequivocally identified first isochrones magnetic anomaly M 25 (154 Ma), would conjointly benefit to the palinspastic reconstruction of the EMS.

Rifting dynamic and comparison to other passive margin systems

As already proposed by Robertson (2007), margins of the EMS do not have characteristic features of magma-rich or magma-poor rifted margins. The EMS passive margin evolution could be summarized as following: 1) pulsated rift activity over wide domains (from Permian to Early Cretaceous); 2) sharp crustal tapering, 3) short-lived spreading system; 4) post rift thermal subsidence with carbonate platform on the continental margin and starved sedimentation in the deep basin. Similar passive margin architectures and poly-phase tectonic evolution are observed in the Eastern Black Sea (EBS) (Monteleone et al. 2019), South China Sea (SCS) (Le Pourhiet et al. 2018; Larsen et al. 2018; Nirrengarten et al. 2020) and Woodlark Basin (Goodliffe and Taylor 2007).

The geodynamic context of opening of those oceanic basins presents similarities with the EMS: 1) In contrast to the Atlantic, these oceanic basins did not form in the middle of a super-continent (Pangea). Instead, they formed along the edges of super-continents, leading to the separation of elongated continental ribbons from larger plates (e.g. Palawan Block; Woodlark Rise) (Wang et al. 2019); 2) The rifted continental lithosphere was initially formed in relation with active margins, the proto-Tethys subduction in the EMS, the proto-Pacific subduction in the SCS and the Paleo-Tethys for the EBS (Okay and Nikishin 2015). This setting will create a particular lithospheric inheritance in terms of structures (folds, thrusts, plutons), rheology (metasedimentary composition, decoupling levels), thermal structure and geochemistry (mantle and crustal), which affect the development of extensional tectonic responses; 3) Active subduction zones are observed in the proximity of all those oceanic basins during their formation (Stephenson and Schellart 2010; Wu and Suppe 2018); 4) The spreading evolution is short-lived, as shown in EBS and SCS (< 20 Ma) (Taylor and Hayes 1983; Monteleone et al. 2019) and was likely similarly short-lived in the EMS (Tugend et al. 2019) (Fig. 12); 5) The direction of rifting and of spreading is variable through time during the formation of such basins (Briais et al. 1993; Le Pourhiet et al. 2018). Without magnetic anomalies or transform faults,

it is therefore problematic to unambiguously interpret the direction of opening of such oceanic marginal basins solely based on the sharpness of the passive margin architecture.

Conclusion

We investigated the rifting evolution of the EMS by combining seismic sections of preserved EMS rifted margin, borehole data, gravity anomaly maps and tectono-stratigraphic information from the northern conjugate margins preserved in fold and thrust belts. This analysis is integrated into a global plate motion model, enabling the identification of potential geodynamic controls on the Mesozoic extension of the EMS. We point out that a better calibration of the dynamic of the early Mesozoic subductions zone in the NE of the EMS and of the early Central Atlantic opening are needed to tackle the evolution of the EMS.

The main conclusions are as follow:

1. A new structural rift domain map of the EMS is proposed and accompanied by four regional seismic cross sections through different margin segments. This map highlights the different morphology of the Herodotus and northern Levant oceanic basin compared to the structured highly thinned continental crust flooring the southern Levant Basin.
2. Based on offshore borehole observations and the integration of the stratigraphy of the potential conjugate margins, we propose a deformation timeline as follows: a Late Triassic opening of the northern Levant basin, an Early to Middle Jurassic rifting and spreading of the Western Desert margin and Herodotus Basin. At the junction of these two segments, the southern Levant basin represents an aborted rift system characterized by a poly-phased extension from Permian to Middle Jurassic.
3. EMS rifted margins have a sharp crustal taper interpreted as the narrow juxtaposition between thinned continental crust and oceanic crust. This characteristic feature is similar to other marginal sea rifted margins systems such as EBS, SCS.
4. The EMS rifting evolution is poly-phased and multiple breakup ages are identified. The exact direction of opening could not be determined in the absence of kinematic markers. However, the size of the EMS and its structural complexity suggest multiple variations in geodynamic regime through Mesozoic in relation with the Tethyan subductions and the Central Atlantic opening.

Supplementary Information The online version contains supplementary material available at https://doi.org/10.1007/s00531-022-02263-5.

Acknowledgements We are grateful to PGS and TGS for getting access to the publication of high-quality seismic figures. This work was funded by Total through a postdoc grant to M.N. This work benefited from fruitful discussions with the people of Total MENA exploration team. We thank our academics colleagues and in particular S. Schmid for all the discussions on the regional geology. We also would like to thank the editorial handling by W.C. Dullo and C. Hübscher and the constructive reviews by two anonymous reviewers.

References

Abadi AM, van Wees JD, van Dijk PM, Cloetingh SAPL (2008) Tectonics and subsidence evolution of the Sirt Basin, Libya. Am Assoc Pet Geol Bull 92:993–1027. https://doi.org/10.1306/03310806070

Abd-Allah AMA, El-Naby AA, Abdel Aal MH (2001) Tectonic and basin evolution of South Eastern Mediterranean for hydrocarbon potentiality in North Sinai. Egypt J Pet Sci Eng 190:107080. https://doi.org/10.1016/j.petrol.2020.107080

Abd El-Fattah BK, Moustafa AR, Yousef M (2021) A new insight into the structural evolution of Rosetta Fault, eastern margin of Herodotus Basin. East Mediterranean Mar Pet Geol 131:105161. https://doi.org/10.1016/j.marpetgeo.2021.105161

Al-Riyami K, Robertson A (2002) Mesozoic sedimentary and magmatic evolution of the Arabian continental margin, northern Syria: evidence from the Baer-Bassit Melange. Geol Mag 139:395–420. https://doi.org/10.1017/S0016756802006660

Al-Saad D, Sawaf T, Gebran A et al (1992) Crustal structure of central Syria: the intracontinental Palmyride mountain belt. Tectonophysics 207:345–358. https://doi.org/10.1016/0040-1951(92)90395-M

Allen H, Jackson CAL, Fraser AJ (2016) Gravity-driven deformation of a youthful saline giant: the interplay between gliding and spreading in the Messinian basins of the Eastern Mediterranean. Pet Geosci 22:340–356. https://doi.org/10.1144/petgeo2016-034

Amante C, Eakins BW (2009) ETOPO1 1 Arc-Minute Global Relief Model: Procedures, Data Sources and Analysis

Arsenikos S, Frizon De Lamotte D, Chamot-Rooke N et al (2013) Mechanism and timing of tectonic inversion in Cyrenaica (Libya): integration in the geodynamics of the East Mediterranean. Tectonophysics 608:319–329. https://doi.org/10.1016/j.tecto.2013.09.025

Arsenikos S (2014) Tectonic evolution and structure of the Cyrenaica margin, Libya (East Mediterranean). Université de Cergy Pontoise Arsenikos S (2014) Tectonic evolution and structure of the Cyrenaica margin, Libya (East Mediterranean). Université de Cergy Pontoise

Arthaud F, Matte P (1977) Late paleo-strike-slip faulting in S-Europe and N-Africa: results of a right-lateral shear zone between the Appalachians and the Urals. Geol Soc Am Bull 88:1305–1320. https://doi.org/10.1130/0016-7606(1977)88%3c1305:LPSFIS%3e2.0.CO;2

Auboin J (1959) Contribution à l'étude géologique de la Grèce septentrionale: les confins de l'Epire et de la Thessalie. Ann Géol Pays Hell X:483

Avigad D, Abbo A, Gerdes A (2016) Origin of the eastern mediterranean: neotethys rifting along a cryptic cadomian suture with Afro-Arabia. Bull Geol Soc Am 128:1286–1296. https://doi.org/10.1130/B31370.1

Avigad D, Kolodner K, McWilliams M et al (2003) Origin of northern Gondwana Cambrian sandstone revealed by detrital zircon SHRIMP dating. Geology 31:227–230. https://doi.org/10.1130/0091-7613(2003)031%3c0227:OONGCS%3e2.0.CO;2

Barrier E, Machhour L, Blaizot M (2014) Petroleum systems of Syria. AAPG Mem 106:335–378. https://doi.org/10.1036/13431862M1063612

Basilone L, Frixa A, Trincianti E, Valenti V (2016) Permian-Cenozoic deep-water carbonate rocks of the Southern Tethyan Domain. The case of Central Sicily. Ital J Geosci 135:171–198. https://doi.org/10.3301/IJG.2015.07

Ben-Avraham Z, Ginzburg A, Makris J, Eppelbaum L (2002) Crustal structure of the Levant Basin, eastern Mediterranean. Tectonophysics 346:23–43. https://doi.org/10.1016/S0040-1951(01)00226-8

Ben-Avraham Z, Grasso M (1991) Crustal structure variations and transcurrent faulting at the eastern and western margins of the eastern Mediterranean. Tectonophysics 196:269–277. https://doi.org/10.1016/0040-1951(91)90326-N

Ben-Avraham Z, Woodside J, Lodolo E et al (2006) Eastern Mediterranean basin systems. Geol Soc Mem 32:263–276. https://doi.org/10.1144/GSL.MEM.2006.032.01.15

Ben-Gai Y (2019) Internal structure of the triangular horst-like Jonah high in the Levant basin. Eastern Mediterranean Search Discov. https://doi.org/10.1306/11257Ben-Gai2019

Best JA, Muawia B, Al-Saad D et al (1993) Continental margin evolution of the Northern Arabian Platform in Syria. Am Assoc Pet Geol Bull. https://doi.org/10.1306/BDFF8BBE-1718-11D7-8645000102C1865D

Beydoun ZR (1977) Petroleum prospects of Lebanon: reevaluation. Am Assoc Pet Geol Bull. https://doi.org/10.1306/C1EA3BF4-16C9-11D7-8645000102C1865D

Biju-Duval B (1983) Depressions circulaires au pied de l'escarpement de Malte et morphologie des escarpements sous-marins. Problemes d'interpretation. Rev - Inst Fr Du Pet 38:605–619. https://doi.org/10.2516/ogst:1983036

Bizon G, Muller C, Vieban F (1985) Les sédiments mésozoïques et cénozoïques de mer Ionienne (campagne Escarmed 3: escarpement de Malte, mont Alfeo et monts de Médine). Etude biostratigraphique : foraminifères, nannoplancton, microfaciès. Rev L'institut Français Du Pétrole 40:431–455. https://doi.org/10.2516/ogst:1985027

Blakely RJ (1995) Potential theory in gravity and magnetic applications. Cambridge University Press

Bosworth W, El-Hawat AS, Helgeson DE, Burke K (2008) Cyrenaican "shock absorber" and associated inversion strain shadow in the collision zone of northeast Africa. Geology 36:695–698. https://doi.org/10.1130/G24909A.1

Bosworth W, Guiraud R, Kessler LG (1999) Late Cretaceous (ca. 84 Ma) compressive deformation of the stable platform of northeast Africa (Egypt): far-field stress effects of the "Santonian event" and origin of the Syrian arc deformation belt. Geology 27:633–636. https://doi.org/10.1130/0091-7613(1999)027%3c0633:LCCMCD%3e2.3.CO;2

Bosworth W, Huchon P, McClay K (2005) The Red Sea and Gulf of Aden Basins. J African Earth Sci 43:334–378. https://doi.org/10.1016/j.jafrearsci.2005.07.020

Bowman SA (2011) Regional seismic interpretation of the hydrocarbon prospectivity of offshore Syria. GeoArabia 16:95–124

Brew G, Barazangi M, Al-Maleh AK, Sawaf T (2001) Tectonic and geologic evolution of Syria. GeoArabia 6:573–616

Briais A, Patriat P, Tapponnier P (1993) Updated interpretation of magnetic anomalies and seafloor spreading stages in the south China Sea: Implications for the Tertiary tectonics of Southeast Asia. J Geophys Res Solid Earth 98:6299–6328. https://doi.org/10.1029/92JB02280

Buiter SJH, Torsvik TH (2014) A review of Wilson Cycle plate margins: A role for mantle plumes in continental break-up along sutures? Gondwana Res 26:627–653. https://doi.org/10.1016/j.gr.2014.02.007

Caméra L, Ribodetti A, Mascle J (2010) Deep structures and seismic stratigraphy of the Egyptian continental margin from multichannel seismic data. Geol Soc Spec Publ 341:85–97. https://doi.org/10.1144/SP341.5

Carton H, Singh SC, Tapponnier P et al (2009) Seismic evidence for Neogene and active shortening offshore of Lebanon (Shalimar cruise). J Geophys Res Solid Earth. https://doi.org/10.1029/2007JB005391

Chamot-Rooke N, Rangin C, Le Pichon X, Group D working (2005) DOTMED : Deep Offshore Tectonics of the Mediterranean. A synthesis of deep marine data in the eastern Mediterranean, Mémoires. Paris, France

Channell JET, Kozur HW (1997) How many oceans? Meliata, Vardar, Pindos oceans in Mesozoic Alpine paleogeography. Geology 25:183–186. https://doi.org/10.1130/0091-7613(1997)025%3c0183:HMOMVA%3e2.3.CO;2

Ciarapica G, Passeri L (2002) The palaeogeographic duplicity of the Apennines. Boll Della Soc Geol Ital 1:67–75

Cowie L, Kusznir N (2012a) Mapping crustal thickness and oceanic lithosphere distribution in the eastern Mediterranean using gravity inversion. Pet Geosci 18:373–380. https://doi.org/10.1144/petgeo2011-071

Cowie L, Kusznir N (2012b) Gravity inversion mapping of crustal thickness and lithosphere thinning for the eastern Mediterranean. Lead Edge 31:810–814. https://doi.org/10.1190/tle31070810.1

Dellong D, Klingelhoefer F, Kopp H et al (2018) Crustal Structure of the Ionian Basin and Eastern Sicily Margin: Results From a Wide-Angle Seismic Survey. J Geophys Res Solid Earth 123:2090–2114. https://doi.org/10.1002/2017JB015312

Dercourt J, Zonenshain LP, Ricou L-E et al (1986) Geological evolution of the Tethys belt from the Atlantic to the Pamirs since the LIAS. Tectonophysics 123(1–4):241–315

Dercourt J, Ricou L-E, Vrielynck B (1993) Atlas Tethys palaeoenvironmental maps, Gauthier-V. Paris, France

Dewey JF, Bird JM (1970) Mountain belts and the new global tectonics. J Geophys Res 75:2625–2647. https://doi.org/10.1029/JB075i014p02625

Dewey JF, Helman ML, Knott SD et al (1989) Kinematics of the western Mediterranean. Geol Soc London, Spec Publ 45:265–283. https://doi.org/10.1144/GSL.SP.1989.045.01.15

de Voogd B, Truffert C, Chamot-Rooke N et al (1992) Two-ship deep seismic soundings in the basins of the Eastern Mediterranean Sea (Pasiphae cruise). Geophys J Int 109:536–552. https://doi.org/10.1111/j.1365-246X.1992.tb00116.x

Dolson JC, Shann MV, Matbouly SI et al (2001) Egypt in the twenty-first century: petroleum potential in offshore trends. GeoArabia 6:211–230

Druckman Y (1974) Triassic paleogeography of southern Israel and the Sinai Peninsula. Die Stratigraphie der alpin-mediterranen Trias/The Stratigraphy of the Alpine-Mediterranean Triassic. Springer, Vienna, pp 79–86

Druckman Y, Hirsch F, Weissbrod T (1982) The Triassic of the southern margin of the Tethys in the Levant and its correlation across the Jordan Rift Valley. Geol Rundschau 71:919–936. https://doi.org/10.1007/BF01821111

Dubertret L (1966) Liban, Syrie et bordure des pays voisins. Première partie, Tableau stratigraphique avec carte géologique au millionième. Paris

El-Sharkawy A, Meier T, Hübscher C et al (2021) Lithospheric structure of the eastern Mediterranean Sea: inferences from surface wave tomography and stochastic inversions constrained by wide-angle refraction measurements. Tectonophysics 821:229159. https://doi.org/10.1016/j.tecto.2021.229159

Faccenna C, Becker TW, Auer L et al (2014) Mantle dynamics in the Mediterranean. Rev Geophys 52(3):283–332

Feld C, Mechie J, Hübscher C et al (2017) Crustal structure of the Eratosthenes Seamount, Cyprus and S. Turkey from an amphibian wide-angle seismic profile. Tectonophysics 700–701:32–59. https://doi.org/10.1016/j.tecto.2017.02.003

Ferriere J, Baumgartner PO, Chanier F (2016) The Maliac Ocean: the origin of the Tethyan Hellenic ophiolites. Int J Earth Sci 105:1941–1963. https://doi.org/10.1007/s00531-016-1303-6

Ferrière J, Chanier F, Ditbanjong P (2012) The Hellenic ophiolites: eastward or westward obduction of the Maliac Ocean, a discussion. Int J Earth Sci 101:1559–1580. https://doi.org/10.1007/s00531-012-0797-9

Fleury JJ (1980) Les zones de Gavrovo-Tripolitza et du Pinde_Olonos: Evolution d'une plate-forme et d'un bassin dans leur cadre alpin. Université Lilles1- Sciences et Technologies

Fritz H, Abdelsalam M, Ali KA et al (2013) Orogen styles in the East African Orogen: A review of the Neoproterozoic to Cambrian tectonic evolution. J African Earth Sci 86:65–106. https://doi.org/10.1016/j.jafrearsci.2013.06.004

Frizon de Lamotte D, Raulin C, Mouchot N et al (2011) The southernmost margin of the Tethys realm during the Mesozoic and Cenozoic: Initial geometry and timing of the inversion processes. Tectonics. https://doi.org/10.1029/2010tc002691

Frizon De Lamotte D, Tavakoli-Shirazi S, Leturmy P et al (2015) Evidence for Late Devonian vertical movements and extensional deformation in northern Africa and Arabia: integration in the geodynamics of the Devonian world. Tectonics 32:107–122. https://doi.org/10.1002/tect.20007

Gardosh M, Druckman Y, Buchbinder B, Rybakov M (2008) The Levant Basin Offshore Israel: Stratigraphy, Structure, Tectonic Evolution and Implications for Hydrocarbon Exploration - revised edition. Geological Survey of Israel report GSI/4/2008. 121

Gardosh MA, Druckman Y (2006) Seismic stratigraphy, structure and tectonic evolution of the Levantine Basin, offshore Israel. Geol Soc Spec Publ 260:201–227. https://doi.org/10.1144/GSL.SP.2006.260.01.09

Gardosh MA, Garfunkel Z, Druckman Y, Buchbinder B (2010) Tethyan rifting in the Levant Region and its role in Early Mesozoic crustal evolution. Geol Soc Spec Publ 341:9–36. https://doi.org/10.1144/SP341.2

Gardosh MA, Tannebaum E (2014) The petroleum systems of the Levant Basin. L Marlow, C Kendall L Yose, eds, Pet Syst Tethyan Reg AAPG Mem 106:179–216. https://doi.org/10.1036/13431857M106298

Garfunkel Z (2015) The relations between Gondwana and the adjacent peripheral Cadomian domain-constrains on the origin, history, and paleogeography of the peripheral domain. Gondwana Res 28:1257–1281. https://doi.org/10.1016/j.gr.2015.05.011

Garfunkel Z (1998) Constrains on the origin and history of the Eastern Mediterranean basin. Tectonophysics 298:5–35. https://doi.org/10.1016/S0040-1951(98)00176-0

Garfunkel Z, Derin B (1984) Permian-early Mesozoic tectonism and continental margin formation in Israel and its implications for the history of the Eastern Mediterranean. Geol Soc Spec Publ 17:187–201. https://doi.org/10.1144/GSL.SP.1984.017.01.12

Gawlick H-J, Missoni S, Suzuki H et al (2016) Triassic radiolarite and carbonate components from a Jurassic ophiolitic mélange (Dinaridic Ophiolite Belt). Swiss J Geosci 109:473–494. https://doi.org/10.1007/s00015-016-0232-5

Ghalayini R, Nader FH, Bou Daher S et al (2018) Petroleum systems of Lebanon: an update and review. J Pet Geol 41:189–214. https://doi.org/10.1111/jpg.12700

Golan T, Katzir Y, Coble MA (2021) The timing of rifting events in the easternmost Mediterranean: U-Pb dating of zircons from volcanic rocks in the Levant margin. Int Geol Rev. https://doi.org/10.1080/00206814.2021.1955416

Goodliffe AM, Taylor B (2007) The boundary between continental rifting and sea-floor spreading in the Woodlark Basin, Papua New Guinea. Geol Soc London, Spec Publ 282:217–238. https://doi.org/10.1144/SP282.11

Granot R (2016) Palaeozoic oceanic crust preserved beneath the eastern Mediterranean. Nat Geosci 9:701–705. https://doi.org/10.1038/ngeo2784

Hawie N, Gorini C, Deschamps R et al (2013) Tectono-stratigraphic evolution of the northern Levant Basin (offshore Lebanon). Mar Pet Geol 48:392–410. https://doi.org/10.1016/j.marpetgeo.2013.08.004

Jagger LJ, Bevan TG, McClay KR (2020) Tectono-stratigraphic evolution of the se mediterranean passive margin, offshore egypt and libya. Geol Soc Spec Publ 476:365–401. https://doi.org/10.1144/SP476.10

Jolivet L, Faccenna C, Goffé B et al (2003) Subduction tectonics and exhumation of high-pressure metamorphic rocks in the Mediterranean orogens. Am J Sci 303:353–409. https://doi.org/10.2475/ajs.303.5.353

Kellner A, Brink GJ, El Khawaga H (2018) Depositional history of the western Nile Delta, Egypt: Late Rupelian to Pleistocene. Am Assoc Pet Geol Bull 102:1841–1865. https://doi.org/10.1306/02161817234

Keppie DF (2015) How the closure of paleo-Tethys and Tethys oceans controlled the early breakup of Pangaea. Geology 43:335–338. https://doi.org/10.1130/G36268.1

King MT, Welford JK, Cadenas P, Tugend J (2021) Investigating the plate kinematics of the Bay of Biscay using deformable plate tectonic models. Tectonics 40(7):e2020TC006467

Kozur H (1991) The evolution of the Meliata-Hallstatt ocean and its significance for the early evolution of the Eastern Alps and Western Carpathians. Paleogeography, Palaeoclimatol Palaeoecol 87:108–135

Larsen HC, Mohn G, Nirrengarten M et al (2018) Rapid transition from continental breakup to igneous oceanic crust in the South China Sea. Nat Geosci 11:782–789. https://doi.org/10.1038/s41561-018-0198-1

Laubscher H, Bernoulli D (1977) Mediterranean and Tethys. Ocean Basins Margins. https://doi.org/10.1007/978-1-4684-3036-3_1

Le Pichon X, Lemoine AMC, İmren C (2019) A new approach to the opening of the eastern mediterranean sea and the origin of the hellenic subduction zone. Part 1: T The eastern Mediterranean Sea. Can J Earth Sci 56:1119–1143. https://doi.org/10.1139/cjes-2018-0128

Le Pourhiet L, Chamot-Rooke N, Delescluse M et al (2018) Continental break-up of the South China Sea stalled by far-field compression. Nat Geosci. https://doi.org/10.1038/s41561-018-0178-5

Lemoine M (1983) Rifting and Early Drifting: Mesozoic Central Atlantic and Ligurian Tethys. In: Initial Reports of the Deep Sea Drilling Project, 76. U.S. Government Printing Office

Lemoine M, Bas T, Arnaud-Vanneau A, Arnaud H, Dumont T, Gidon M, Tricart P (1986) The continental margin of the Mesozoic Tethys in the Western Alps. Mar Pet Geol 3(3):179–199

Longacre M, Bentham P, Hanbal I, et al (2007) New Crustal Structure of the Eastern Mediterranean Basin: Detailed Integration and Modeling of Gravity, Magnetic, Seismic Refraction, and Seismic Reflection Data. In: EGM 2007 International Workshop. European Association of Geoscientists & Engineers

Loncke L, Gaullier V, Mascle J et al (2006) The Nile deep-sea fan: An example of interacting sedimentation, salt tectonics, and inherited subsalt paleotopographic features. Mar Pet Geol 23:297–315. https://doi.org/10.1016/j.marpetgeo.2006.01.001

Macgregor DS (2012) The development of the Nile drainage system: integration of onshore and offshore evidence. Pet Geosci 18:417–431. https://doi.org/10.1144/petgeo2011-074

Makris J, Ben AZ, Behle A et al (1983) Seismic refraction profiles between Cyprus and Israel and their interpretation. Geophys J R Astron Soc 75:575–591. https://doi.org/10.1111/j.1365-246X.1983.tb05000.x

Masini E, Manatschal G, Mohn G et al (2011) The tectono-sedimentary evolution of a supra-detachment rift basin at a deep-water magma-poor rifted margin: The example of the Samedan Basin preserved in the Err nappe in SE Switzerland. Basin Res 23:652–677. https://doi.org/10.1111/j.1365-2117.2011.00509.x

Matte P (2001) The Variscan collage and orogeny (480–290 Ma) and the tectonic definition of the Armorica microplate: a review. Terra Nov 13:122–128

McKenzie D (1972) Active Tectonics of the Mediterranean Region. Geophys J R Astron Soc 30:109–185. https://doi.org/10.1111/j.1365-246X.1972.tb02351.x

McKenzie DP (1984) The generation and compaction of partial melts. J Petrol 25:713–765

Mechie J, Abu-ayyash K, Ben-Avraham Z et al (2009) Crustal structure of the southern Dead Sea basin derived from project DESIRE wide-angle seismic data. Geophys J Int 178:457–478. https://doi.org/10.1111/j.1365-246X.2009.04161.x

Menant A, Jolivet L, Vrielynck B (2016) Kinematic reconstructions and magmatic evolution illuminating crustal and mantle dynamics of the eastern Mediterranean region since the late Cretaceous. Tectonophysics 675:103–140. https://doi.org/10.1016/j.tecto.2016.03.007

Meyer B, Saltus R, Chulliat A (2017) EMAG2: Earth Magnetic Anomaly Grid (2-arc-minute resolution) Version 3

Missoni S, Gawlick HJ, Sudar MN et al (2012) Onset and demise of the Wetterstein Carbonate Platform in the mélange areas of the Zlatibor Mountain (Sirogojno, SW Serbia). Facies 58:95–111. https://doi.org/10.1007/s10347-011-0274-0

Mohn G, Manatschal G, Müntener O et al (2010) Unravelling the interaction between tectonic and sedimentary processes during lithospheric thinning in the Alpine Tethys margins. Int J Earth Sci 99:75–101. https://doi.org/10.1007/s00531-010-0566-6

Moix P, Vachard D, Allibon J et al (2013) Palaeotethyan, Neotethyan and Hu Lu-Pindos Series in the Lycian Nappes (Sw Turkey): Geodynamical Implications. New Mex Museum Nat Hist Bull 61:401–444

Monteleone V, Minshull TA, Marin-Moreno H (2019) Spatial and temporal evolution of rifting and continental breakup in the eastern black sea basin revealed by long-offset seismic reflection data. Tectonics 38:2646–2667. https://doi.org/10.1029/2019TC005523

Moustafa AR (2008) Mesozoic-Cenozoic basin evolution in the Northern Western Desert of Egypt. Geol East Libya 3:29–46

Moustafa AR (2010) Structural setting and tectonic evolution of North Sinai folds. Egypt Geol Soc Spec Publ 341:37–63. https://doi.org/10.1144/SP341.3

Moustafa AR, Fouda HGA (2014) Structural architecture and tectonic evolution of the Yelleg inverted half graben, northern Sinai. Egypt Mar Pet Geol 51:286–297. https://doi.org/10.1016/j.marpetgeo.2014.01.001

Moustafa AR (2020) Mesozoic-Cenozoic Deformation History of Egypt. In: akaria Hamimi, Dr. Ahmed El-Barkooky, Prof. Dr. Jesús Martínez Frías, Prof. Harald Fritz DYAE-R (ed) The Geology of Egypt, Regional G. pp 253–290

Müller RD, Zahirovic S, Williams SE et al (2019) A Global plate model including lithospheric deformation along major rifts and orogens since the triassic. Tectonics 38(6):1884–1907

Muttoni G, Dallanave E, Channell JET (2013) The drift history of Adria and Africa from 280Ma to Present, Jurassic true polar wander, and zonal climate control on Tethyan sedimentary facies. Palaeogeogr Palaeoclimatol Palaeoecol 386:415–435. https://doi.org/10.1016/j.palaeo.2013.06.011

Nader FH, Inati L, Ghalayini R et al (2018) Key geological characteristics of the Saida-Tyr Platform along the eastern margin of the Levant Basin, offshore Lebanon: implications for hydrocarbon exploration. Oil Gas Sci Technol. https://doi.org/10.2516/ogst/2018045

Netzeband GL, Gohl K, Hübscher CP et al (2006) The Levantine Basin-crustal structure and origin. Tectonophysics 418:167–188. https://doi.org/10.1016/j.tecto.2006.01.001

Nirrengarten M, Manatschal G, Tugend J et al (2018) Kinematic Evolution of the Southern North Atlantic: implications for the Formation of Hyperextended Rift Systems. Tectonics. https://doi.org/10.1002/2017TC004495

Nirrengarten M, Mohn G, Schito A et al (2020) The thermal imprint of continental breakup during the formation of the South China Sea. Earth Planet Sci Lett. https://doi.org/10.1016/j.epsl.2019.115972

Okay AI, Nikishin AM (2015) Tectonic evolution of the southern margin of Laurasia in the Black Sea region. Int Geol Rev 57:1051–1076. https://doi.org/10.1080/00206814.2015.1010609

Ozsvárt P, Dumitrica P, Moix P (2019) New early Late Carnian (Upper Triassic) radiolarians from the Pindos-Huğlu succession of the South-Taurides ophiolite belt. Swiss J Geosci 112:251–266. https://doi.org/10.1007/s00015-018-0326-3

Palano M, Ferranti L, Monaco C et al (2012) GPS velocity and strain fields in Sicily and southern Calabria, Italy: updated geodetic constraints on tectonic block interaction in the central Mediterranean. J Geophys Res Solid Earth 117:1–12. https://doi.org/10.1029/2012JB009254

Papadimitriou N, Gorini C, Nader FH et al (2018) Tectono-stratigraphic evolution of the western margin of the Levant Basin (offshore Cyprus). Mar Pet Geol 91:683–705. https://doi.org/10.1016/j.marpetgeo.2018.02.006

Peace AL, Welford JK, Ball PJ, Nirrengarten M (2019) Deformable plate tectonic models of the southern North Atlantic. J Geodyn. https://doi.org/10.1016/j.jog.2019.05.005

Peron-Pinvidic G, Manatschal G, Osmundsen PT (2013) Structural comparison of archetypal Atlantic rifted margins:a review of observations and concepts. Mar Pet Geol 43:21–47. https://doi.org/10.1016/j.marpetgeo.2013.02.002

Petersen KD, Schiffer C (2016) Wilson cycle passive margins: control of orogenic inheritance on continental breakup. Gondwana Res 39:131–144. https://doi.org/10.1016/j.gr.2016.06.012

Poisson A (1984) The extension of the Ionian trough into southwestern Turkey. Geol Soc London, Spec Publ 17:241–249. https://doi.org/10.1144/GSL.SP.1984.017.01.18

Ranero CR, Pérez-Gussinyé M (2010) Sequential faulting explains the asymmetry and extension discrepancy of conjugate margins. Nature 468:294–299. https://doi.org/10.1038/nature09520

Reilinger R, McClusky S, Vernant P et al (2006) GPS constraints on continental deformation in the Africa-Arabia-Eurasia continental collision zone and implications for the dynamics of plate interactions. J Geophys Res Solid Earth 111:1–26. https://doi.org/10.1029/2005JB004051

Reston TJ (2009) The structure, evolution and symmetry of the magma-poor rifted margins of the North and Central Atlantic: a synthesis. Tectonophysics 468:6–27. https://doi.org/10.1016/j.tecto.2008.09.002

Ring U, Layer PW, Reischmann T (2001) Miocene high-pressure metamorphism in the Cyclades and Crete, Aegean Sea, Greece: Evidence for large-magnitude displacement on the Cretan detachment. Geology 29:395–398. https://doi.org/10.1130/0091-7613(2001)029%3c0395:MHPMIT%3e2.0.CO;2

Roberts G, Peace D (2007) Hydrocarbon plays and prospectivity of the Levantine Basin, offshore Lebanon and Syria from modern seismic data. GeoArabia 12:99–124. https://doi.org/10.3997/2214-4609.20146462

Robertson A, Shallo M (2000) Mesozoic-Tertiary tectonic evolution of Albania in its regional Eastern Mediterranean context. Tectonophysics 316:197–254. https://doi.org/10.1016/S0040-1951(99)00262-0

Robertson AHF (2007) Overview of tectonic settings related to the rifting and opening of Mesozoic ocean basins in the Eastern Tethys: Oman, Himalayas and Eastern Mediterranean regions. Geol Soc Spec Publ 282:325–388. https://doi.org/10.1144/SP282.15

Robertson AHF (1998) Formation and destruction of the Eratosthenes Seamount, eastern Mediterranean Sea, and implications for collisional processes. Proc Ocean Drill Progr Sci Results 160:681–700. https://doi.org/10.2973/odp.proc.sr.160.063.1998

Robertson AHF (2006) Sedimentary evidence from the south Mediterranean region (Sicily, Crete, Peloponnese, Evia) used to test alternative models for the regional tectonic setting of Tethys during Late Palaeozoic - Early Mesozoic time. Geol Soc Spec Publ 260:91–154. https://doi.org/10.1144/GSL.SP.2006.260.01.06

Robertson AHF, Dixon JE, Brown S et al (1996) Alternative tectonic models for the Late Palaeozoic-Early Tertiary development of Tethys in the Eastern Mediterranean region. Geol Soc Spec Publ 105:239–263. https://doi.org/10.1144/GSL.SP.1996.105.01.22

Robertson AHF, Mountrakis D (2006) Tectonic development of the Eastern Mediterranean region: An introduction. Geol Soc Spec Publ 260:1–9. https://doi.org/10.1144/GSL.SP.2006.260.01.01

Robertson AHF, Parlak O, Rízaoğlu T et al (2007) Tectonic evolution of the South Tethyan ocean: Evidence from the Eastern Taurus Mountains (Elaziğ region, SE Turkey). Geol Soc Spec Publ 272:231–270. https://doi.org/10.1144/GSL.SP.2007.272.01.14

Rosenbaum G, Lister GS, Duboz C (2002) Relative motions of Africa, Iberia and Europe during Alpine orogeny. Tectonophysics 359:117–129. https://doi.org/10.1016/S0040-1951(02)00442-0

Roveri M, Gennari R, Lugli S et al (2016) The Messinian salinity crisis: open problems and possible implications for Mediterranean petroleum systems. Pet Geosci 22:283–290. https://doi.org/10.1144/petgeo2015-089

Rusciadelli G, Shiner P (2018) Isolated carbonate platforms of the Mediterranean and their seismic expression — Searching for a paradigm. Lead Edge 37:492–501. https://doi.org/10.1190/tle37070492.1

Sagy Y, Gvirtzman Z, Reshef M (2018) 80 m.y. of folding migration: New perspective on the Syrian arc from Levant Basin analysis. Geology 46:175–178. https://doi.org/10.1130/G39654.1

Sandwell DT, Müller RD, Smith WHF et al (2014) New global marine gravity model from CryoSat-2 and Jason-1 reveals buried tectonic structure. Science (80-) 346:65–67. https://doi.org/10.1126/science.1258213

Sapin F, Ringenbach JC, Clerc C (2021) Rifted margins classification and forcing parameters. Sci Rep. https://doi.org/10.1038/s41598-021-87648-3

Savva D, Pubellier M, Franke D et al (2014) Different expressions of rifting on the South China Sea margins. Mar Pet Geol 58:579–598. https://doi.org/10.1016/j.marpetgeo.2014.05.023

Schattner U, Ben-Avraham Z (2007) Transform margin of the northern Levant, eastern Mediterranean: From formation to reactivation. Tectonics 26:1–17. https://doi.org/10.1029/2007TC002112

Schmid SM, Fügenschuh B, Kounov A et al (2020) Tectonic units of the Alpine collision zone between Eastern Alps and western Turkey. Gondwana Res 78:308–374. https://doi.org/10.1016/j.gr.2019.07.005

Segev A, Rybakov M (2010) Effects of Cretaceous plume and convergence, and Early Tertiary tectonomagmatic quiescence on the central and southern Levant continental margin. J Geol Soc London 167:731–749. https://doi.org/10.1144/0016-76492009-118

Segev A, Rybakov M (2011) History of faulting and magmatism in the Galilee (Israel) and across the Levant continental margin inferred from potential field data. J Geodyn 51:264–284. https://doi.org/10.1016/j.jog.2010.10.001

Segev A, Sass E, Schattner U (2018) Age and structure of the Levant basin, Eastern Mediterranean. Earth-Sci Rev 182:233–250. https://doi.org/10.1016/j.earscirev.2018.05.011

Sengor AMC (1990) Plate-Tectonics and Orogenic research after 25 years - a Tethyan perspective. Earth-Sci Rev 27:1–201

Şengör AMC, Yilmaz Y (1981) Tethyan evolution of Turkey: aplate tectonic approach. Tectonophysics 75:181–241. https://doi.org/10.1016/0040-1951(81)90275-4

Şengör AMC, Yilmaz Y, Sungurlu O (1984) Tectonics of the Mediterranean Cimmerides: nature and evolution of the western termination of Palaeo-Tethys. Geol Soc Spec Publ 17:77–112. https://doi.org/10.1144/GSL.SP.1984.017.01.04

Sibila Borojević Š, Franz N, Robert H, Ladislav AP (2012) Tectonothermal history of the basement rocks within the NW Dinarides: New40 Ar/39 Ar ages and synthesis. Geol Carpathica 63:441–452. https://doi.org/10.2478/v10096-012-0034-2

Sobh M, Ebbing J, Mansi AH, Götze HJ (2019) Inverse and 3D forward gravity modelling for the estimation of the crustal thickness of Egypt. Tectonophysics 752:52–67. https://doi.org/10.1016/j.tecto.2018.12.002

Spahic D, Glavas-Trbic B, Djajic S, Gaudenyi T (2018) Neoproterozoic-paleozoic evolution of the Drina formation (Drina-Ivanjica entity). Geol Anal Balk Poluostrva 79:57–68. https://doi.org/10.2298/GABP1802057S

Stampfli GM, Borel GD (2002) A plate tectonic model for the Paleozoic and Mesozoic constrained by dynamic plate boundaries and restored syntetic ocean isochrons. Earth Planet Sci Lett 196:17–33. https://doi.org/10.1016/S0012-821X(01)00588-X

Stampfli GM, Borel GD (2004) The TRANSMED transects in space and time: constraints on the paleotectonic evolution of the Mediterranean domain. The TRANSMED atlas. The Mediterranean region from crust to mantle. Springer, Berlin, Heidelberg, pp 53–80

Stampfli GM, Kozur HW (2006) Europe from the Variscan to the Alpine cycles. Geol Soc Mem 32:57–82. https://doi.org/10.1144/GSL.MEM.2006.032.01.04

Steinberg J, Roberts AM, Kusznir NJ et al (2018) Crustal structure and post-rift evolution of the Levant Basin. Mar Pet Geol 96:522–543. https://doi.org/10.1016/j.marpetgeo.2018.05.006

Stephan T, Kroner U, Romer RL (2019) The pre-orogenic detrital zircon record of the Peri-Gondwanan crust. Geol Mag 156:281–307. https://doi.org/10.1017/S0016756818000031

Stephenson R, Schellart WP (2010) The black Sea back-arc basin: Insights to its origin from geodynamic models of modern analogues. Geol Soc Spec Publ 340:11–21. https://doi.org/10.1144/SP340.2

Sudar MN, Gawlick HJ, Lein R et al (2013) Depositional environment, age and facies of the Middle Triassic Bulog and rid formations in the Inner Dinarides (Zlatibor Mountain, SW Serbia): Evidence for the Anisian break-up of the Neotethys Ocean. Neues Jahrb Fur Geol Und Palaontologie - Abhandlungen 269:291–320. https://doi.org/10.1127/0077-7749/2013/0352

Symeou V, Homberg C, Nader FH et al (2018) Longitudinal and temporal evolution of the tectonic style along the Cyprus arc system, assessed through 2-D reflection seismic interpretation. Tectonics 37:30–47. https://doi.org/10.1002/2017TC004667

Tari G, Hussein H, Novotny B et al (2012) Play types of the deep-water Matruh and Herodotus Basins, NW Egypt. Pet Geosci 18:443–455. https://doi.org/10.1144/petgeo2012-011

Tari G, Arbouille D, Schléder Z, Tóth T (2020) Inversion tectonics: a brief petroleum industry perspective. Solid Earth 11:1865–1889. https://doi.org/10.5194/se-11-1865-2020

Tassy A, Crouzy E, Gorini C et al (2015) Egyptian Tethyan margin in the Mesozoic: evolution of a mixed carbonate-siliciclastic shelf

edge (from Western Desert to Sinai). Mar Pet Geol 68:565–581. https://doi.org/10.1016/j.marpetgeo.2015.10.011

Taylor B, Hayes D (1983) Origin and history of the South China Sea basin. In: Hayes D (eds) The Tectonic and Geologic Evolution of Southeast Asian Seas and Islands: Part 2. pp 23–56

Torley JM, Robertson AHF (2018) New evidence and interpretation of facies, provenance and geochemistry of late Triassic-early Cretaceous Tethyan deep-water passive margin-related sedimentary rocks (Ayios Photios Group), SW Cyprus in the context of eastern Mediterranean geodynamics. Sediment Geol 377:82–110. https://doi.org/10.1016/j.sedgeo.2018.09.001

Tugend J, Manatschal G, Kusznir NJ et al (2014) Formation and deformation of hyperextended rift systems: Insights from rift domain mapping in the Bay of Biscay-Pyrenees. Tectonics 33:1239–1276. https://doi.org/10.1002/2014TC003529

Tugend J, Manatschal G, Kusznir NJ (2015a) Spatial and temporal evolution of hyperextended rift systems: Implication for the nature, kinematics, and timing of the Iberian- European plate boundary. Geology 43:15–18. https://doi.org/10.1130/G36072.1

Tugend J, Manatschal G, Kusznir NJ, Masini E (2015b) Characterizing and identifying structural domains at rifted continental margins: application to the Bay of Biscay margins and its Western Pyrenean fossil remnants. Geol Soc London, Spec Publ 413:171–203. https://doi.org/10.1144/SP413.3

Tugend J, Chamot-Rooke N, Arsenikos S et al (2019) Geology of the ionian basin and margins: a key to the east mediterranean geodynamics. Tectonics 38(8):2668–2702

van Hinsbergen DJJ, Torsvik TH, Schmid SM et al (2020) Orogenic architecture of the Mediterranean region and kinematic reconstruction of its tectonic evolution since the Triassic. Gondwana Res 81:79–229. https://doi.org/10.1016/j.gr.2019.07.009

Van Simaeys S, Janszen A, Hardy C, et al (2019) Unravelling the tectono-stratigraphy of the Eratosthenes continental block. In: 81st EAGE Conf Exhib 2019. https://doi.org/10.3997/2214-4609.201900906

Warrlich G, Bosence D, Waltham D et al (2008) 3D stratigraphic forward modelling for analysis and prediction of carbonate platform stratigraphies in exploration and production. Mar Pet Geol 25:35–58. https://doi.org/10.1016/j.marpetgeo.2007.04.005

Wang P, Huang CY, Lin J et al (2019) The South China Sea is not a mini-Atlantic: plate-edge rifting vs intra-plate rifting. Natl Sci Rev 6:902–913. https://doi.org/10.1093/nsr/nwz135

Welford JKK, Hall J, Hübscher C et al (2015) Crustal seismic velocity structure from Eratosthenes Seamount to Hecataeus Rise across the Cyprus Arc, eastern Mediterranean. Geophys J Int 200:933–951. https://doi.org/10.1093/gji/ggu447

Whitmarsh RB, Manatschal G, Minshull TA (2001) Evolution of magma-poor continental margins from rifting to seafloor spreading. Nature 413:150–154. https://doi.org/10.1038/35093085

Wu J, Suppe J (2018) Proto-South China Sea plate tectonics using subducted slab constraints from tomography. J Earth Sci 29:1304–1318. https://doi.org/10.1007/s12583-017-0813-x

Ye Q, Mei L, Shi H et al (2018) A low-angle normal fault and basement structures within the Enping Sag, Pearl River Mouth Basin: Insights into late Mesozoic to early Cenozoic tectonic evolution of the South China Sea area. Tectonophysics 731–732:1–16. https://doi.org/10.1016/j.tecto.2018.03.003

Yousef M, Moustafa AR, Shann M (2010) Structural Setting and Tectonic Evolution of Offshore North Sinai, Egypt. Geol Soc, London, Spec Publ 341(1):65–84. https://doi.org/10.1144/SP341.4